

4-23-2008

Provenance Analysis of the Cretaceous Pythian Cave Conglomerate, Northern California

Gregory Alan Augsburg
Trinity University

Follow this and additional works at: http://digitalcommons.trinity.edu/geo_honors



Part of the [Earth Sciences Commons](#)

Recommended Citation

Augsburger, Gregory Alan, "Provenance Analysis of the Cretaceous Pythian Cave Conglomerate, Northern California" (2008).
Geosciences Student Honors Theses. 3.
http://digitalcommons.trinity.edu/geo_honors/3

This Thesis open access is brought to you for free and open access by the Geosciences Department at Digital Commons @ Trinity. It has been accepted for inclusion in Geosciences Student Honors Theses by an authorized administrator of Digital Commons @ Trinity. For more information, please contact jcostanz@trinity.edu.

Provenance Analysis of the Cretaceous Pythian Cave Conglomerate, Northern California

Gregory Alan Augsburg

A departmental senior thesis submitted to the Department of Geosciences at Trinity University in partial fulfillment of the requirements for graduation with departmental honors.

April 23, 2008

Dr. Kathleen D. Surpless
Thesis Advisor

Dr. Glenn Kroeger
Department Chair

Michael Fischer
Associate Vice President
for
Academic Affairs

Student Copyright Declaration: the author has selected the following copyright provision (select only one):

This thesis is licensed under the Creative Commons Attribution-NonCommercial-NoDerivs License, which allows some noncommercial copying and distribution of the thesis, given proper attribution. To view a copy of this license, visit <http://creativecommons.org/licenses/> or send a letter to Creative Commons, 559 Nathan Abbott Way, Stanford, California 94305, USA.

This thesis is protected under the provisions of U.S. Code Title 17. Any copying of this work other than "fair use" (17 USC 107) is prohibited without the copyright holder's permission.

Other:

Table of Contents

Table of Contents	1
List of Figures.....	2
Abstract	3
Introduction	5
Geologic Setting	10
The Cordilleran Orogen	10
Klamath Mountains	13
Sierra Nevadas	15
Hornbrook Formation.....	15
Field Methodology.....	16
The Pythian Cave Conglomerate.....	17
Zircon Methodology.....	25
Results	27
Geochronology	27
Geochemistry.....	32
Discussion.....	34
Conclusions.....	36
Acknowledgements.....	38
References.....	39
Appendix.....	42

LIST OF FIGURES

Figure 1. Reconstruction of the Cordilleran Terranes.....	6
Figure 2. Overview of Klamath Mountain Terranes.....	8
Figure 3. Location Map.....	18
Figure 4. Stratigraphic Column with Rose Diagrams.....	20
Figure 5. Clast Composition Plots.....	22
Figure 6. Field photos showing cobble orientation.....	23
Figure 7. QFL Diagram.....	23
Figure 8. Sandstone petrography.....	24
Figure 9. Cobble petrography 1.....	24
Figure 10. Cobble petrography 2.....	25
Figure 11. Detrital Zircon Data: Normalized curves.....	28
Figure 12. Detrital Zircon Data: Cumulative probability curves.....	29
Figure 13. Igneous Zircon Data: Best fit ages.....	30
Figure 14. Igneous Zircon Data: Age vs. Uranium concentration.....	31
Figure 15. Major Element Geochemistry: Total Alkali vs. Silica.....	33
Figure 16. Trace Element Geochemistry: Spider Diagram.....	33

ABSTRACT

Reconstructions of the Mesozoic paleogeography of the North American Cordillera depend on data that can link displaced terranes to each other and/or to the North American craton. The Pythian Cave Conglomerate (PCC) sits unconformably on the eastern terranes of the Klamath Mountains south of Yreka, California and has the potential to yield valuable information about the tectonic history of the region. The PCC is approximately 60 m thick, with the lower 40 m dominated by cobble conglomerate with thin sandstone lenses, and the upper 20 m containing thicker and more laterally continuous interbedded sandstone layers. Originally interpreted as Tertiary conglomerate based on petrologic similarity to other Tertiary units in the region, the PCC was dated as Albian (112 – 99 Ma) by a later pollen study. The youngest detrital zircon age peak in the PCC of 131 Ma provides a maximum depositional age and is consistent with Albian deposition. Paleoflow readings from cobble imbrication and sandstone cross bedding suggest that the source of the sediment was to the east-northeast. Thin-section petrography of cobbles throughout the PCC indicates a source dominated by hydrothermally-altered intermediate volcanic rocks, consistent with sandstone point-counts that plot in the arc and dissected arc provenance fields. Detrital zircon age spectra and conglomerate clast counts are consistent throughout the entire PCC section, implying a uniform provenance. Two PCC sandstone samples both yield two distinct detrital zircon age peaks of Early/Middle Jurassic (165-190 Ma) and Early Cretaceous (130-150 Ma), with few Late Jurassic (150-165 Ma) detrital zircon grains. Four igneous clasts also yield an Early Jurassic age. Together, these results suggest a proximal magmatic arc source to

the east-northeast of the PCC that was active in Early-Middle Jurassic and Early Cretaceous time and may now be buried under Tertiary volcanic rocks. Youngest detrital zircon ages of 131 Ma, a lack of zircon ages older than 200 Ma, along with a southwesterly paleoflow, disqualify the Klamath Mountains as a source. These results indicate a potential source for the PCC in the northern Sierra Nevada Mountains or a now-buried northern continuation of the Sierra Nevada Mountains.

Introduction

The provenance of sedimentary rocks can help with reconstructing the tectonic history of a complex region by delimiting the amount of tectonic motion of the sedimentary basin relative to its source since deposition. Characterizing sediment provenance can support or discredit various paleogeographic reconstructions that position a basin adjacent to different source regions. Eliminating potential sources if they do not fit provenance data, or qualifying them if they do fit provenance data, helps provide motion constraints for the PCC.

During the late Mesozoic Era, the Cordilleran Mountains of the western United States were characterized by two distinct geological regions (e.g., Cowan and Bruhn, 1992, and references therein). The eastern region was characterized by a thin-skinned fold and thrust belt and a resulting foreland basin, while the western region was dominated by subduction of oceanic crust resulting in magmatic arcs with forearc and backarc basin systems (Cowan and Bruhn, 1992, and references therein). From the latest Mesozoic on, major tectonic deformation has disrupted the potentially once-continuous basin systems in this western region, resulting in more “localized sedimentation” (Miller et al., 1992). Many of the basin deposits preserved today in the Cordillera are disconnected from their sediment sources, and some hypotheses suggest displacement of

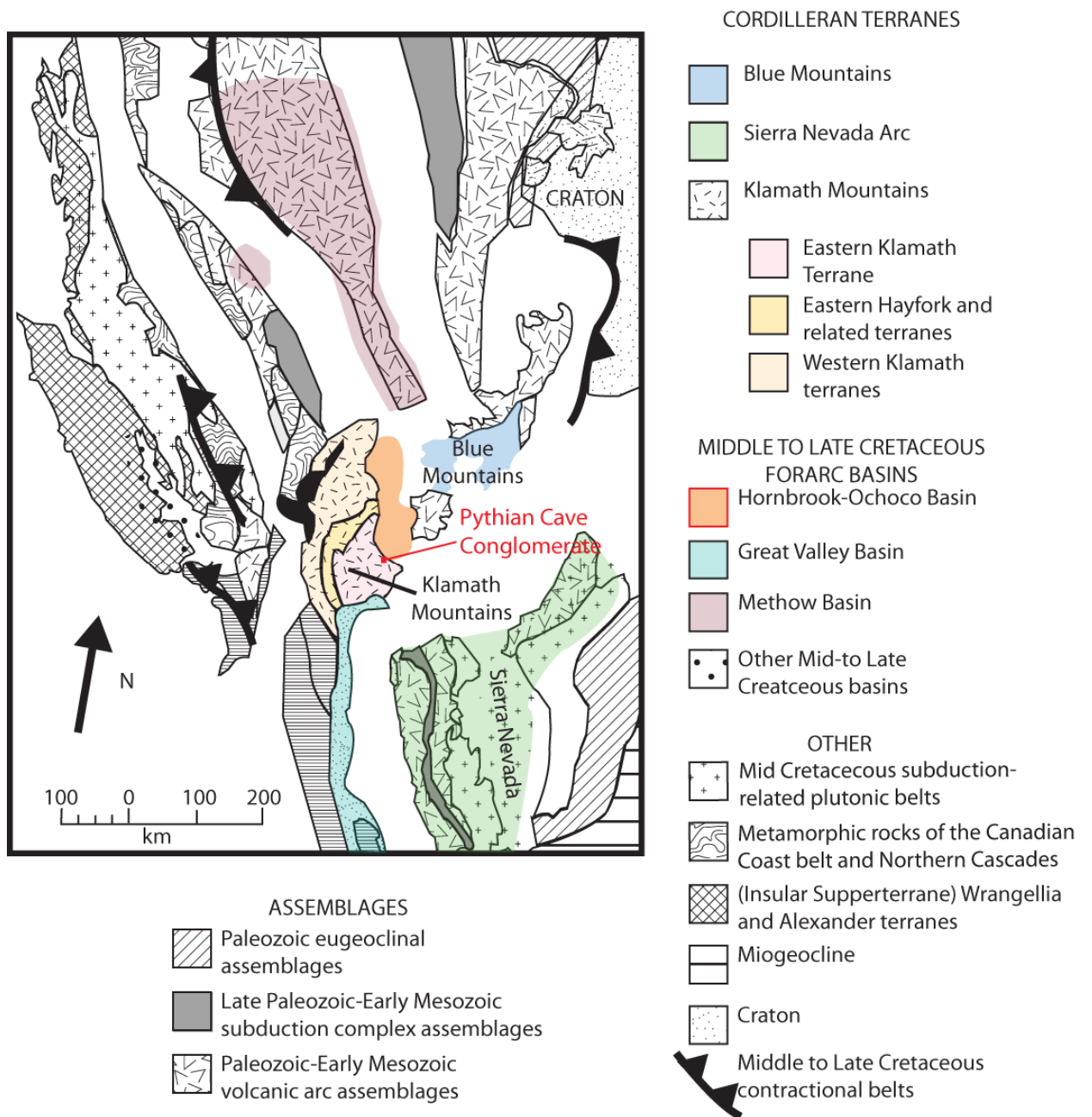


Figure 1. Local Cordilleran terranes surrounding the Pythian Cave Conglomerate in the minimum offset model of Wyld and others (2006).

the basins ranging from 1000-3000+ kilometers since deposition (summarized in Wyld et al., 2006).

Interpretations of two differing datasets attempt to reconstruct the Cordilleran tectonics of the Cretaceous Period. One perspective involves significant (>1000 km)

displacement of the Cordilleran terranes since Cretaceous time, while the other supports less motion (<1000 km). Consistent, reproducible paleomagnetic studies suggest thousands of kilometers of northward displacement of the Insular and Intermontane superterranes (Fig. 1) along dextral strike-slip faults during and since the Cretaceous Period (e.g., Irving, 1985). However, structural and stratigraphic field relations along the western margin of North America suggest translation of less than 1000 km along dextral faults (e.g., Wyld et al., 2006).

The multitude of terranes in the Cordilleras, each deformed by a mesh of strike-slip, convergent, and extensional plate motion, makes reconstruction models complex. However, sedimentary rocks can preserve valuable information that has since been lost by burial, erosion, or displacement of crystalline source rocks. The focus of this research is the Pythian Cave Conglomerate (PCC), which lies unconformably on the eastern terranes of the Klamath Mountains south of Yreka, California (Fig. 2; e.g., Jameossanaie and Lindsley-Griffin, 1993). Because the PCC lies atop the Klamath Mountains, any paleogeographic reconstruction with the PCC also implicate the underlying Klamath Mountains to the same terrane translation as the PCC. The PCC has the potential to yield valuable information about the tectonic history of the region for several reasons: 1) the PCC is comprised of large cobbles that suggest close proximity to their source, 2) the conglomerate clasts include felsic plutonic rocks that are useful in age dating, and 3) sandstone layers are interbedded in the conglomerate, permitting source characterization through sediment composition and detrital zircon age data. The PCC was originally interpreted as Tertiary conglomerate based on petrologic similarity to other Tertiary units in the region (Hotz, 1977), but a later pollen study dated the rocks as Albian (112 – 99

Ma; Jameossanaie and Lindsley-Griffin, 1993). Little other work has been done to characterize the source of the PCC and corroborate the Albian age of the PCC.

This investigation reveals valuable provenance information that characterizes a source for the PCC. Age analysis of detrital zircon in three sandstones interbedded in the PCC as well as granite and other felsic clasts provides an Early Cretaceous maximum age of PCC deposition, consistent with pollen data, and helps distinguish ages within the source regions. Zircon age ranges from earliest Jurassic to early Cretaceous, limiting sources to those containing rocks of those specific ages.

Detailed measurement of the stratigraphic section, paleoflow readings from cobble imbrication, clast counts at the top and bottom of the PCC exposure, geochemical analysis of volcanic clasts in the PCC, and point count data from sandstones within the PCC provide abundant additional provenance information. Cobble imbrication readings indicate a paleoflow of S to SW, suggesting the source was located N to NE relative to the PCC during deposition. Clast counts, sandstone petrography, and geochemical analysis of the PCC all point to a volcanic arc setting as a source.

These results suggest a source other than the Klamath Mountains on which the PCC unconformably lies. Combining these provenance data leaves the Sierra Nevada Mountains as the likely source, limited to the older, northern plutons in order to fit the zircon age data. This interpretation advocates placement of the PCC, and the underlying Klamath Mountains terrane, adjacent to the northern Sierra Nevada Mountains or a now-covered northern extension of the Sierra Nevadas in time for Albian deposition (111-98 Ma).

GEOLOGIC SETTING

A knowledge of the regional geology aids in identifying potential source areas and reconstructing tectonic events that may have displaced the basin since deposition. The following overview of the the Cordilleran Orogen and summaries of key attributes of potential sources within the orogen help guide analysis and interpretation of sediment provenance data.

The Cordilleran Orogen

The Cordilleran orogen is home to some of the most complex geology in the world, due to the continental-oceanic plate interactions that have occurred since Cambrian time (e.g., Burchfiel et al., 1992). This long-lived orogeny, which continues today, has resulted from an array of different plate interactions, including convergent, divergent and transform deformation (Burchfiel et al., 1992). The diversity of geology in the region has resulted in the Cordilleras being the focus of intense study by the academic community. Nearly continuous accretion of terranes onto the western margin of North America since the Paleozoic has created a complex geologic picture (e.g., Burchfiel et al., 1992). Older belts have been further deformed by younger belts, through both accretionary and non-accretionary tectonic activity, making reconstruction of the structural evolution of the region particularly difficult (Burchfiel et al., 1992). Despite the concentrated amount of tectonic activity throughout the Phanerozoic in the Cordilleras, large portions of oceanic crust have been preserved and exposed, allowing for reconstruction and modeling of complex structural systems (e.g., Engebretson and others, 1985; Stock and Molnar, 1988).

Ongoing studies (e.g., Irving et al., 1985; Wyld et al., 2006) attempt to reconstruct the paleogeography of regions within the Cordilleras by unraveling tectonic episodes that have deformed the western margin of North America since Paleozoic time. Strong evidence supports the presence of continuous arc systems that formed along a developing western edge of the North American plate (Rubin et al., 1990; Potter et al., 1990). These once-continuous geologic systems have since been heavily deformed, providing clues to the tectonic history since formation of the affected region (Rubin et al., 1990; Potter et al., 1990).

For example, in the Klamath Mountains, Potter et al. (1990) describe evidence of an early Cambrian arc system preserved in the Yreka, Trinity, and eastern Klamath terranes comprised of igneous, metamorphic and sedimentary rocks. The Yreka and eastern Klamath terranes represent a Cambrian arc that evolved into an arc-trench complex dating to mid-Paleozoic time, while the Trinity terrane formed in a back-arc basin of similar age (Potter et al., 1990). Additional biogeographic data suggest that these accreted terranes from that time and region were allochthonous to North America (Potter et al., 1990). Paleomagnetic data indicate plate movement in multiple directions during late Paleozoic time, adding complexity to strike-slip transport scenarios (Mankinen and Irwin, 1990). Contraction and extension events continued through Mesozoic time, resulting in episodic volcanism and metamorphism in the Klamath Mountains (Snoke and Barnes, 2006).

Mankinen and Irwin (1990) use paleomagnetic signatures to reconstruct where the northern Sierra Nevada, Klamath Mountain, and Blue Mountain terranes accreted relative to one another. Mankinen and Irwin (1990) suggest these allochthonous terranes accreted

from south to north, starting with the northern Sierra Nevada terranes, then the Klamath Mountains terranes, and finally the Blue Mountains terranes. Comparing the positions of each terrane at accretion with their modern positions, as reconstructed by Mankinen and Irwin (1990), indicates significant rotation of these terranes since accretion to North America, but no statistically significant latitudinal displacement.

Before attempting to reconstruct possible scenarios of Cretaceous and post-Cretaceous dextral strike-slip movement based on paleomagnetic data, we must first look at known faults, focusing on reconstructing the paleogeography to the closest approximation of the mid-Cretaceous time period through restoration of displacements along contraction and extension belts in the Cordilleras (Wyld et al., 2006). By reconstructing the paleogeography of the Cordillera back to the Cretaceous period using these known and estimated displacements on mapped and hypothesized faults, Wyld et al. (2006) have provided a possible minimum transport distance for testing the Baja B.C. scenarios that postulate much greater transport. Wyld et al.'s (2006) reconstruction indicates a minimum displacement of 900 km to the south of the Insular superterrane, placing the Ochoco and Hornbrook basins adjacent to one another (Fig. 2; Wyld et al., 2006). Additionally, the Intermontane superterrane restores to a position approximately 450 km to 650 km south of its current location (Fig. 2; Wyld et al., 2006).

Both Wyld et al.'s (2006) reconstruction and the Baja B.C. hypothesis suggest large-scale dextral terrane transport within the Cordilleras. The evidence for fault movement within the Cordillera introduces the possibility of displacement of basins away from their sources. By tracing basins back to their sources within the Cordillera, we can gain a better understanding of the tectonics that affected the Cordillera. A more detailed

history of potential sources in the region is necessary to help try to find provenance matches for the PCC. Because zircon is underrepresented in metamorphic assemblages relative to felsic plutonic sources, focusing on plutonic ages of potential sources will better link ages between the source and zircon age data.

Klamath Mountains

The Klamath Mountains formed along the western margin of the North American craton, and are the result of millions of years of accretion (e.g. Snoke and Barnes, 2006). The Klamath Mountains are divided into 4 separate belts of differing ages (Snoke and Barnes, 2006). The oldest accretionary belt, the eastern Klamath belt, contains Paleozoic plutonic ages (Snoke and Barnes, 2006). The most recent magmatic activity occurred in the western Jurassic belts, which were formed by multiple tectonic events during Mesozoic time (Snoke et al., 2006). Earlier interpretations originally constrained the timing of the latest development of the Klamath Mountains from the Late Jurassic into the Early Cretaceous (Harper and Wright, 1984; Schweickert et al., 1984). However, new studies built upon this interpretation and expanded the time constraints for the orogenies associated with creating the Klamath Mountains (Harper et al., 1994).

The tectonic episodes responsible for the most recent activity in the Klamath Mountains fall under two orogenies, the Nevadan Orogeny and the Siskiyou Orogeny (e.g. Hacker and Ernst, 1993). The tectonic setting for these orogenies is still debated, with two leading hypotheses: (1) the Klamath Mountains are a result of collision and subduction (Irwin and Wooden, 1999) or (2) they mainly result from collision and extension (Hacker et al., 1995). The second hypothesis challenges the longstanding theory that the Klamath Mountains were formed by multiple accretions on the western

margin of present day North America, suggesting that “episodic, essentially in situ extension and contraction, rather than accretion, may have built much of the new continental crust” (Hacker et al., 1995).

The Klamath Mountains are composed of multiple east-dipping thrust sheets with west-vergent folds, separated by west-directed thrust faults (Fig. 2; Hacker et al., 1995). The oldest indication of magmatic activity in the Klamath Mountains dates back to approximately 200 Ma (Hacker et al., 1995). Both igneous and metamorphic rocks of this age have been reported throughout the central and western Klamath Mountains, pushing back the initiation of the Klamath Mountains to the Early Jurassic (Hacker et al., 1995). These rocks are referred to as the “Rattlesnake Creek” arc. The early Middle Jurassic (approximately 170 Ma) includes igneous rocks that span nearly the entire length of the Klamath Mountains (Hacker et al., 1995). This “Western Hayfork” arc also is associated with rare metamorphic rocks of the same age, and sedimentary units to the southeast (Hacker et al., 1995). The late Middle Jurassic (167-159 Ma) is characterized by igneous rocks intruded as a result of northwest-trending extension in the central region of the Klamath Mountains (Hacker et al., 1995). The Late Jurassic (approximately 155 Ma) is characterized by northwest-trending magmatism, which migrated to the northern region of the Klamath Mountains (Hacker et al., 1995). From the end of the Jurassic into the Early Cretaceous, the Klamath Mountains had a wide distribution of magmatic activity (Hacker et al., 1995).

Since accretion, the Klamath terranes have rotated about an axis just south of the Yreka terrane (Fig. 2). Wells and others (2000) proposed a rotation of approximately 70° clockwise for the northern Klamath terranes and overlapping Tertiary sediments. This

rotation is significant in provenance interpretations for rocks deposited in the region, as the terrane and their source rock may have been rotated since accretion.

Sierra Nevada Mountains

The Sierra Nevada Mountains resulted from Mesozoic subduction along the western margin of the North American craton (Fig. 3; Schweickert et al., 1984). Plutonic assemblages of felsic composition (Bateman, 1981) make the Sierra Nevada Mountains an excellent supplier of zircon in related basins. The Sierra Nevada Mountains are thought to have originated as a lower crustal magma (Bateman et al., 1963). Magmatism lasted from approximately 210-80 Ma, with magmatism younging to the south (Evernden and Kistler, 1970). The oldest (~210 Ma) magmatism is limited to the eastern side of the batholith, while the western side contains ages of 186-155 Ma (Stern et al., 1981).

Magmatism in the Northern Sierra Nevada coincides with magmatism in the Klamath Mountains associated with the Yreka terrane (Potter et al., 1990). The Shoo Fly Complex includes the northern portion of the Sierra Nevada Mountains, and contains the Lang sequence, Duncan Peak allochthon, Culbertson Lake allochthon, Sierra City Mélange, Sierra Buttes Formation, and the Taylorsville sequence (Schweickert et al., 1984). The Sierra Buttes Formation is dacitic to rhyolitic in composition, while the Taylorsville Formation is andesitic to mafic in composition (Schweickert, 1984; Harwood, 1983).

Hornbrook Formation

The Hornbrook Formation is composed of both non-marine and marine sedimentary rocks representing a period of relative sea level transgression onto the Klamath Mountains during the Late Cretaceous Period (Nilsen, 1993). The formation

crops out in various localities throughout Southern Oregon and Northern California (Fig. 3) and is considered a conformable sedimentary sequence that lies unconformably atop the Klamath Mountains (Nilsen, 1993). The Formation is composed of five members. The oldest member is the Klamath River Conglomerate which is mostly pebble-sized conglomerate and sandstones (Nilsen, 1993). The second member is the Osburger Gulch sandstone, followed by the Ditch Creek Siltstone (3rd), the Rocky Gulch Sandstone (4th), and the Blue Gulch Sandstone (5th) members (Nilsen, 1993).

Like the PCC, the basal unit of the Hornbrook Formation, the Klamath River Conglomerate, also lies unconformably on top of the Klamath Mountains and crops out in the vicinity of the PCC type section. Despite similar age and stratigraphic position, the Klamath River Conglomerate appears to be unrelated to the PCC, as the clasts in the PCC and Klamath River Conglomerate are drastically different in terms of size, clast composition, and the overall conglomerate make-up. The Klamath Mountains are the obvious source for the Klamath River Conglomerate (Nilsen, 1993), so the clear differences between the Klamath River Conglomerate and the PCC suggest that the Klamath Mountains are not the source for the PCC.

FIELD METHODOLOGY

Laboratory work during the 2007 summer and fall semesters involved the isolation of zircon grains from samples collected on site at the PCC outcrop. Additional lab work included thin-section petrography and preparation of samples for geochemical analysis. Field data were collected over a two-week period during the summer of 2007. Data retrieved at outcrops of the PCC near Yreka, California, include two measured stratigraphic sections, grain size and clast size recordings, as well as two clast counts.

Horizontal bedding allowed for the section to be measured using a standard tape measure. Grain size and clast size was measured at each unit, using a grain size card and ruler. One clast count was conducted at the top of the section, the other at the base of the outcrop. The clast counts were performed by sampling grains using a horizontal and vertical spacing equal to the largest cobble size present in the unit, typically 25 centimeters. A sample size of 200 was used for each of the clast counts.

Twenty-six samples of conglomerate cobbles and sandstone were collected at the outcrop and brought back to Trinity University for processing and analysis. Thin-sections were cut for each sample. Of the 26 samples, eight were processed to isolate zircon (four sandstone samples, four felsic igneous cobbles).

THE PYTHIAN CAVE CONGLOMERATE

The Pythian Cave Conglomerate (PCC) crops out approximately 15 km southwest of Yreka, California (Fig. 3), and measures approximately 60 meters in thickness. The PCC was originally thought to be Tertiary river conglomerate that was deposited in a high energy environment close to the sediment source, based on the large, well-rounded cobbles and sand lenses with immature, clay-rich sediment that characterize the PCC (Hotz, 1977; Wetzstein, 1986). The next investigation into the age of the PCC included a pollen taxonomy study that dated the rocks as Albian, 122-99 Ma (Jameossanaie and Lindsley-Griffin, 1993). By comparing palynomorphs from the PCC to palynomorphs in the nearby basal Hornbrook Formation, Jameossanaie and Lindsley-Griffin (1993) concluded the PCC was deposited upstream in a near-source river system, while the basal Hornbrook is interpreted to have been deposited further downstream in a river system.

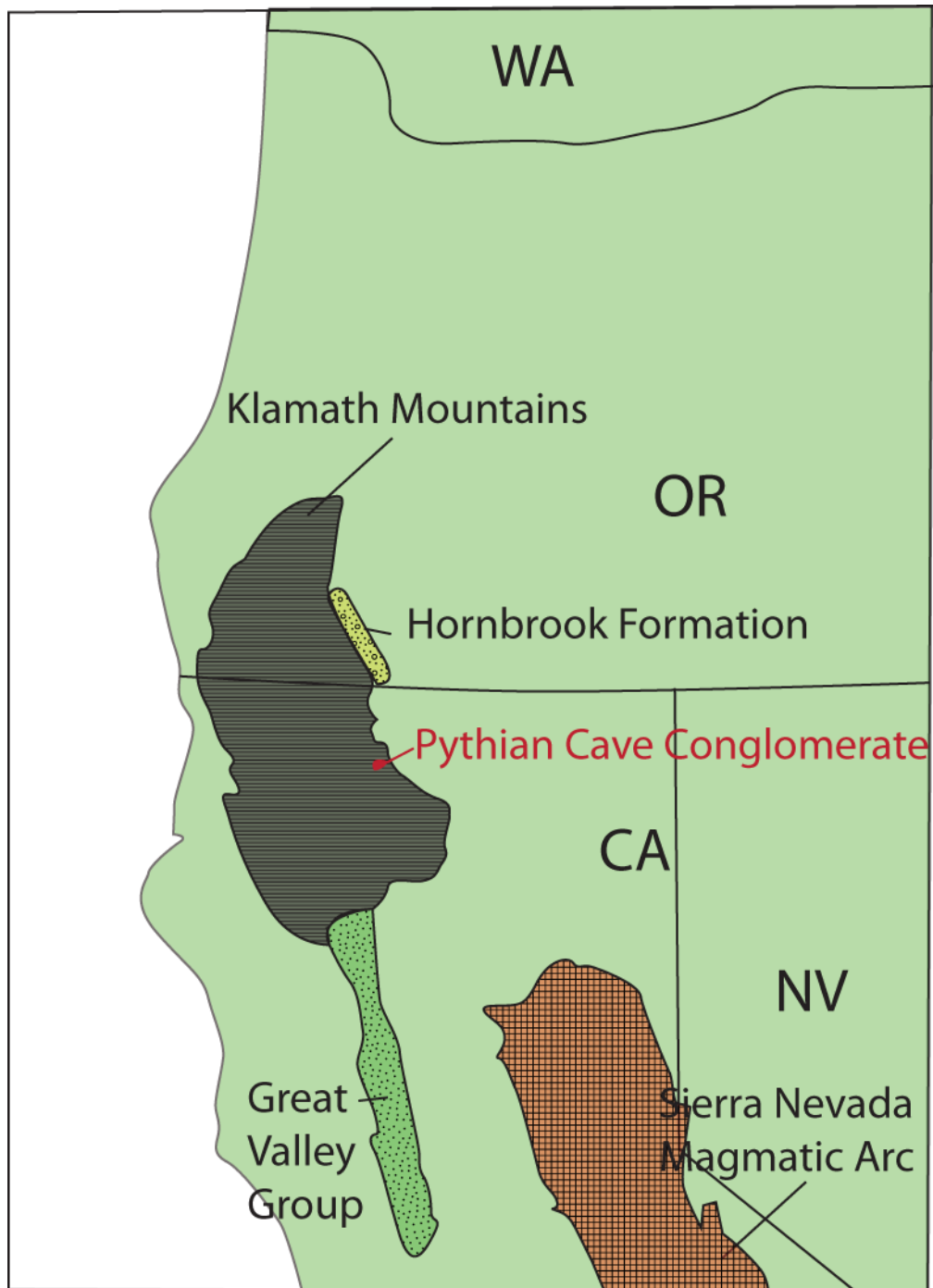


Figure 3. Modern positions of Pythian Cave Conglomerate, Klamath Mountains, Hornbrook Formation, Great Valley Group and Sierra Nevada Magmatic Arc. Figure modified from Snoke and Barnes (2006).

The PCC was previously subdivided into three sections based on clast composition and sandstone regularity (Griffin et al., 1993). Here, the conglomerate is

divided into two sections, based mainly on sandstone frequency. Griffin and others (1993) break out a third subunit based on phyllite and quartzite clasts unique to the highest sections of outcrop. I combine Griffin and others' (1993) second and third subunits into one unit because clast counts indicate no significant change in composition (Figs. 4 and 5).

The lower section (0-40 meters) has thick (up to 10 meters) conglomerate units with thin (approximately 10 centimeters, rarely more than 1 meter), interbedded sand lenses. The majority of the sandstone in the bottom section is mU to cL sand grain size and displays both large-scale and small-scale cross-bedding, with cross-bed thicknesses ranging from several centimeters up to a meter. The cobble sizes average approximately 8-12 centimeters along the long axis, and range from 1 to 30 centimeters. Cobble imbrication is pronounced in the lower section, consistent with Griffin and others' (1993) findings, allowing for paleocurrent data to be collected throughout the lower section (Griffin et al., 1993; Figs. 4 and 6).

The upper section (40-60 meters) contains more frequent sandstone lenses that are relatively thicker than the lower section, ranging from several centimeters to nearly 6 meters thick, and are commonly more than 1 meter thick. The sandstone lenses have similar grain size as in the lower section. Conglomerate cobble sizes in the top section are slightly smaller than in the lower section, with averages of 6-10 centimeters in long axis length and a range of 1-25 centimeters. Cobble orientation becomes chaotic towards the top of the outcrop (Fig. 6).

Conglomerate clast counts conducted in the upper and lower sections yield similar results, with a majority of clasts identified as porphyritic volcanic, consistent with

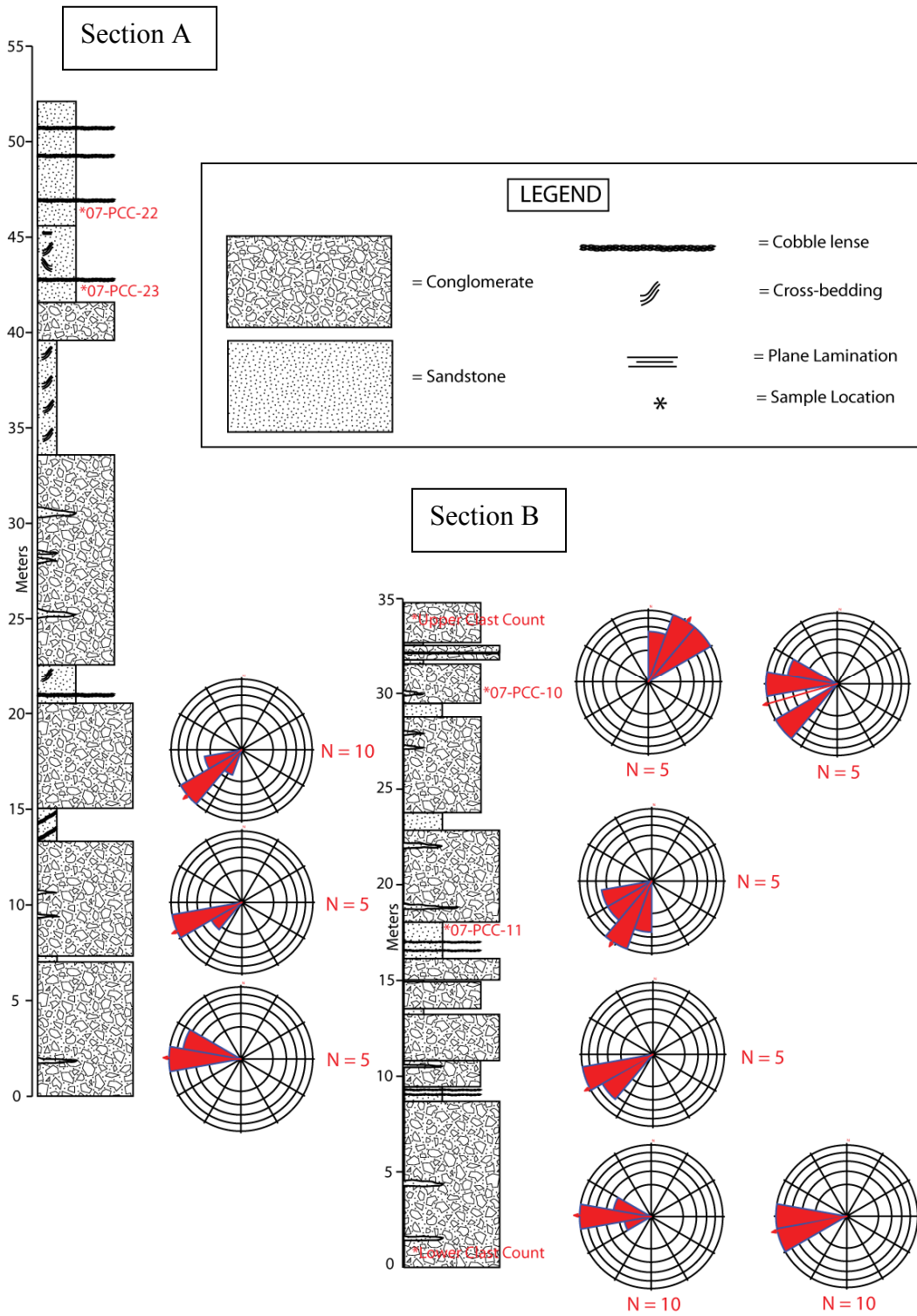


Figure 4. Stratigraphic Column with corresponding paleoflow from imbrication readings. The two sections are separated by a ravine in outcrop, but there is no evidence for fault displacement.

Clast Composition

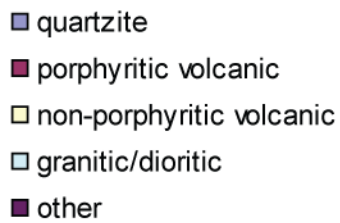
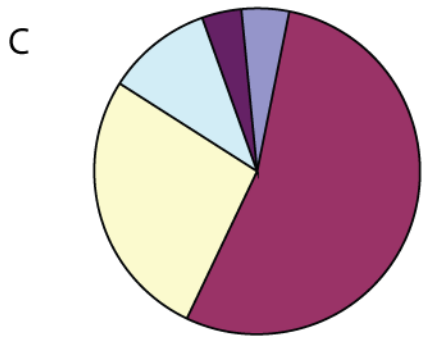
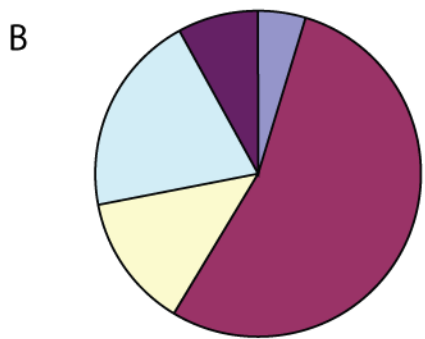
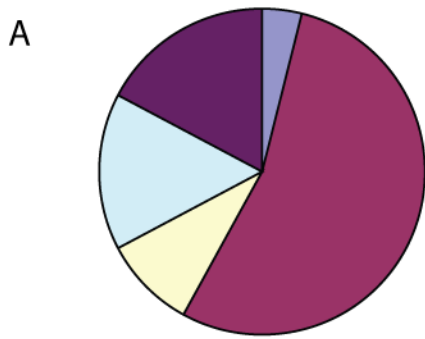


Figure 5. Clast composition plots from the PCC. (A) taken at the top of section B, (B) taken at the bottom of section B, (C) recorded by Wetzstein (1986).



Figure 6. Photos taken at the bottom (A) and top (B) of section B of the PCC outcrop. Notice the well-defined imbrication at the bottom, and the distinctly different chaotic cobble orientation at the top of outcrop.

previous clast counts conducted on the PCC (Wetzstein et al., 1986; Griffin et al., 1993; Fig. 5). Sandstone petrography and point counting also indicate compositional uniformity throughout the PCC exposure. Point-counts of three sandstones, designate similar provenance of a dissected volcanic arc when plotted on a QFL diagram. (Dickinson, 1983; Figs. 7 and 8). This analysis matches those made in previous studies, which suggest a continental arc as the source, based mainly on cobble composition (Wetzstein et al., 1986; Griffin et al., 1993). Cobble petrography revealed intense hydrothermal alteration of volcanic rocks, with some cobbles displaying complete alteration and replacement within the clast (Figs. 9 and 10).

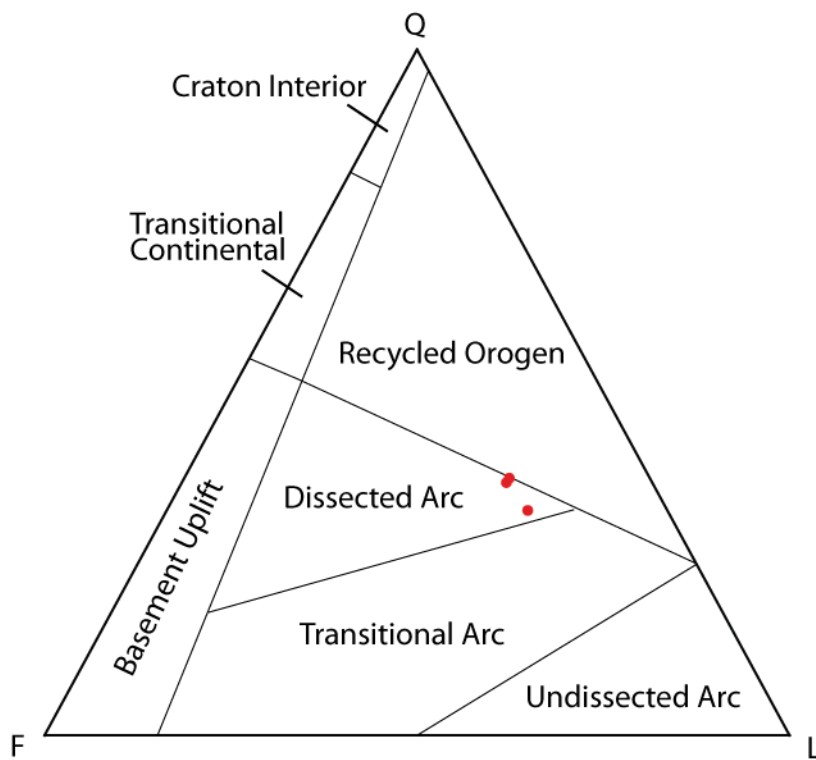


Figure 7. QFL diagram with provenance fields from Dickinson (1993). Point count data (red dots) suggest a dissected arc source for the PCC.

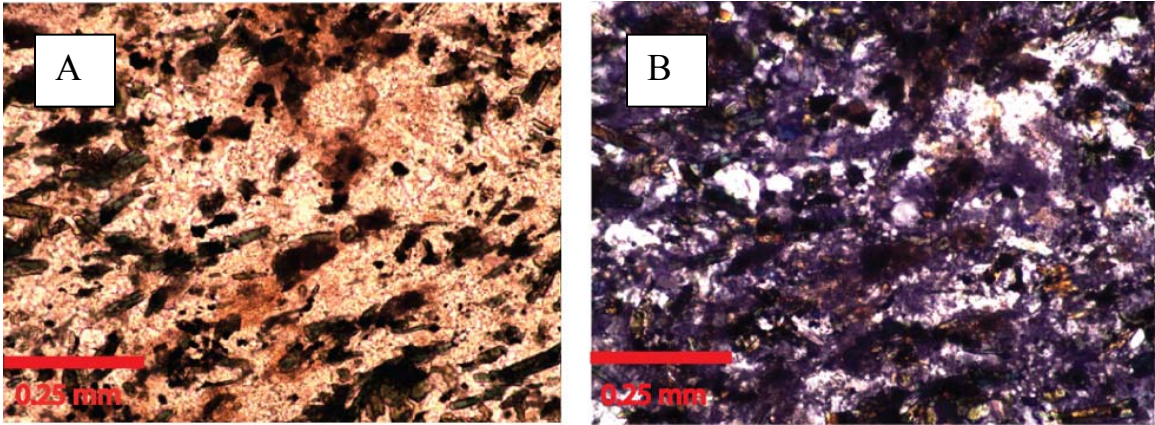


Figure 8. Photomicrographs (20X) of sandstone sample PCC-11 (A = uncrossed polars; B = crossed polars). Notice textural and compositional immaturity (angular grains, high clay content) that help designate a proximal source.

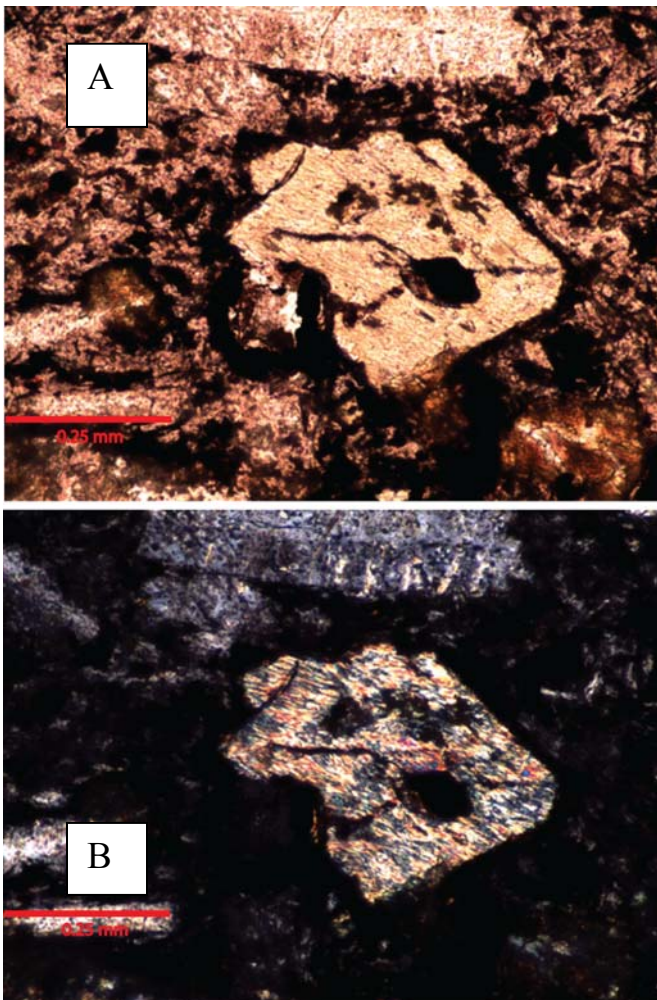


Figure 9. Photomicrographs (20X) of sample PCC-08 (A = uncrossed polars; B = crossed polars) showing distinct cleavage of an amphibole grain with replacement through hydrothermal alteration.

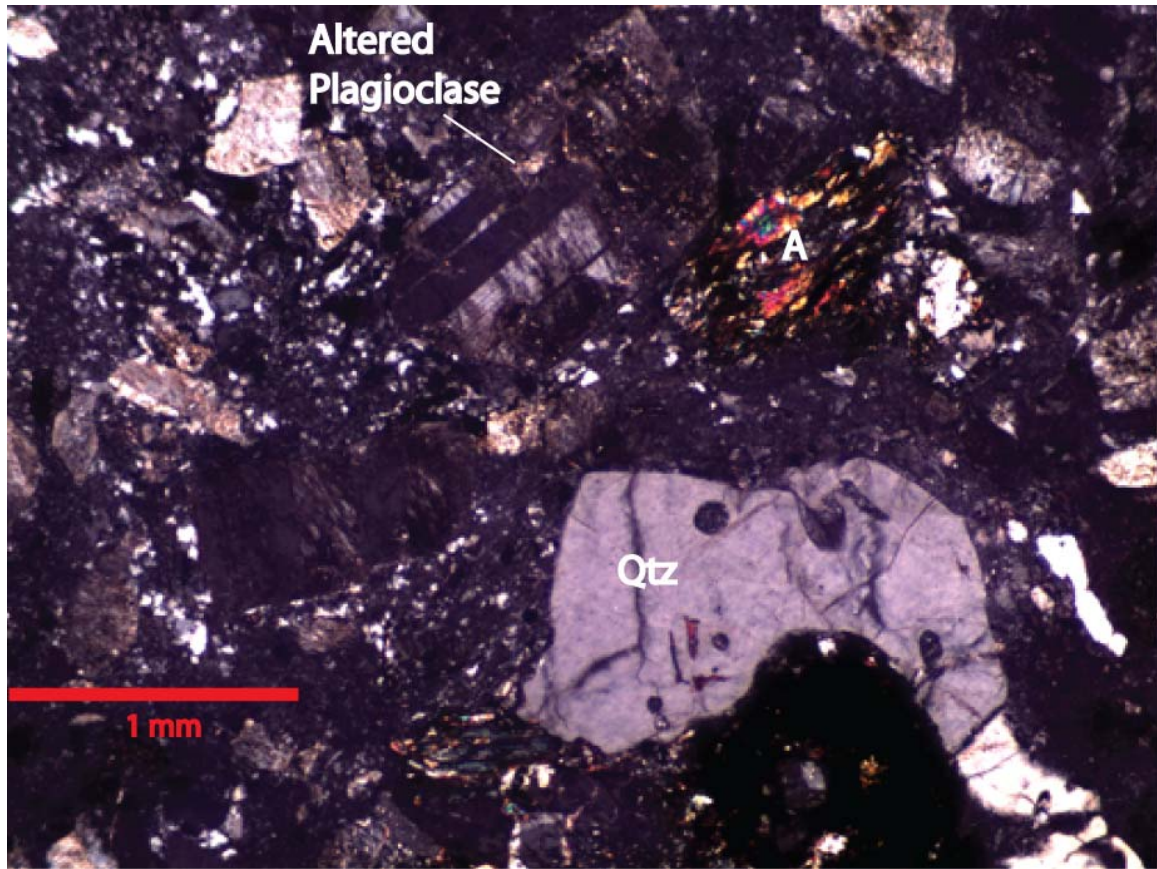


Figure 10. Photomicrographs (5X) of sample PCC-12 under crossed polars showing an amphibole grain (A) along with embayed quartz (Qtz), which is characteristic of quartz in volcanic rocks. Amphibole is key in classifying igneous rocks because it is usually found in intermediate to felsic rocks, and is not a product of hydrothermal alteration.

DETRITAL ZIRCON METHODOLOGY

Zircon isolation included a multi-step procedure, starting with breaking each 1-5 kg sample into smaller pieces using a hammer. The pieces were crushed to approximately pebble size using a rock crusher. The pebbles were then run through a pulverizer that ground them into individual sand grains.

Each sample, now reduced to individual sand grains, was run through a Gemini table to separate the grains based on densities into light and heavy components. Both components were oven-dried. After drying, the light fraction was bagged and labeled and the heavy fraction underwent hand-magnet separation to remove highly magnetic grains,

which were then bagged and labeled. The nonmagnetic heavy fraction was then sieved to remove only the large remaining rock chips. Next, the samples were soaked in 10% acetic acid followed by 3% hydrogen peroxide to remove carbonates and organics, soaking in each solution until reaction stopped. Samples were rinsed thoroughly, and then oven-dried. The sample was then placed in sodium polytungstate (SPT) heavy liquid with a density of 2.84 g/cm³ to further isolate a heavier, zircon-bearing fraction from the lighter material. The lighter material was bagged and labeled. The SPT heavy fraction was then run through a slope Frantz at intervals of 0.3, 0.5, 0.7, and 1.0 amperes. The slope Frantz was set at a back slope of 25 degrees, and a side slope of 20 degrees. The magnetic material was bagged and labeled after each interval. The remaining non-magnetic sample was then processed through methylene iodide heavy liquid of density 3.89 g/cm³. The final separation was then picked to remove pyrite and other remaining non-zircon grains, isolating a pure zircon split. Pure zircon splits were poured two to a slide onto tape, which held grains in place until an epoxy mold was poured. Next, the samples were sanded to approximately half-way through the zircon grains and polished. Exposed zircon grains were then ready for zircon age analysis at the LaserChron Center at the University of Arizona in Tucson.

Using the Laser-Ablation Multicollector ICP Mass Spectrometer, we analyzed three sandstone samples and 4 felsic igneous samples for U-Pb ages of zircon grains. Standard grains of Sri Lankan zircon (SL3) are mounted with the sample and have a known age, allowing for calibration of the machine against the known age to ensure accurate data measurement. We analyzed a standard grain after every five data points for sandstone samples, and after every four data points for igneous samples, following the

procedure of Gehrels and Juiz (2007). Ideally, 100 grains were dated per sandstone sample and 30 grains per igneous clast. However, discordant data points and insufficient zircon reduced that number for several samples. Of the three sandstones, KS-05 produced 102 valid data points, PCC-10 produced 23, and PCC-11 produced 89 data points. I include the age data from 06-KS-05, collected from the PCC in the summer of 2006 and processed in the Laser Chron Center in July 2007. Of the volcanic samples, PCC-04 produced 21 data points, PCC-24 produced 27 data points, PCC-25 produced 25 data points, and PCC-26 produced 29 data points. Grain ages with greater than 5% discordance were discarded. Additionally, igneous zircon grains were checked for differing core and rim ages. No grains were rejected based on core-rim age dissimilarity.

RESULTS

Geochronology

Plotting the detrital zircon age data for PCC sandstone samples using normalized density probability graphs highlights six age peaks across three samples (Fig. 11). The first four age peaks are at 199 Ma, 185 Ma, 177 Ma, and 166 Ma, and contain less than 15 data points comprising each peak. The fifth peak at 143 Ma is significantly larger, containing over 60 grains. The youngest peak is 131 Ma (including 12 grains). The displayed curves account for inherent errors in each data point by summing the Gaussian distribution for each age analysis and associated uncertainty. Also, a normalized distribution of zircon ages for each of the three samples helps visualization of the trends and similarities between samples by keeping a consistent area under the curve for each data set (Fig. 11). In a cumulative probability graph (Fig. 12), steep slopes indicate a

concentration of ages at a specific range, while areas of horizontal slope indicate no zircon grains of that age range.

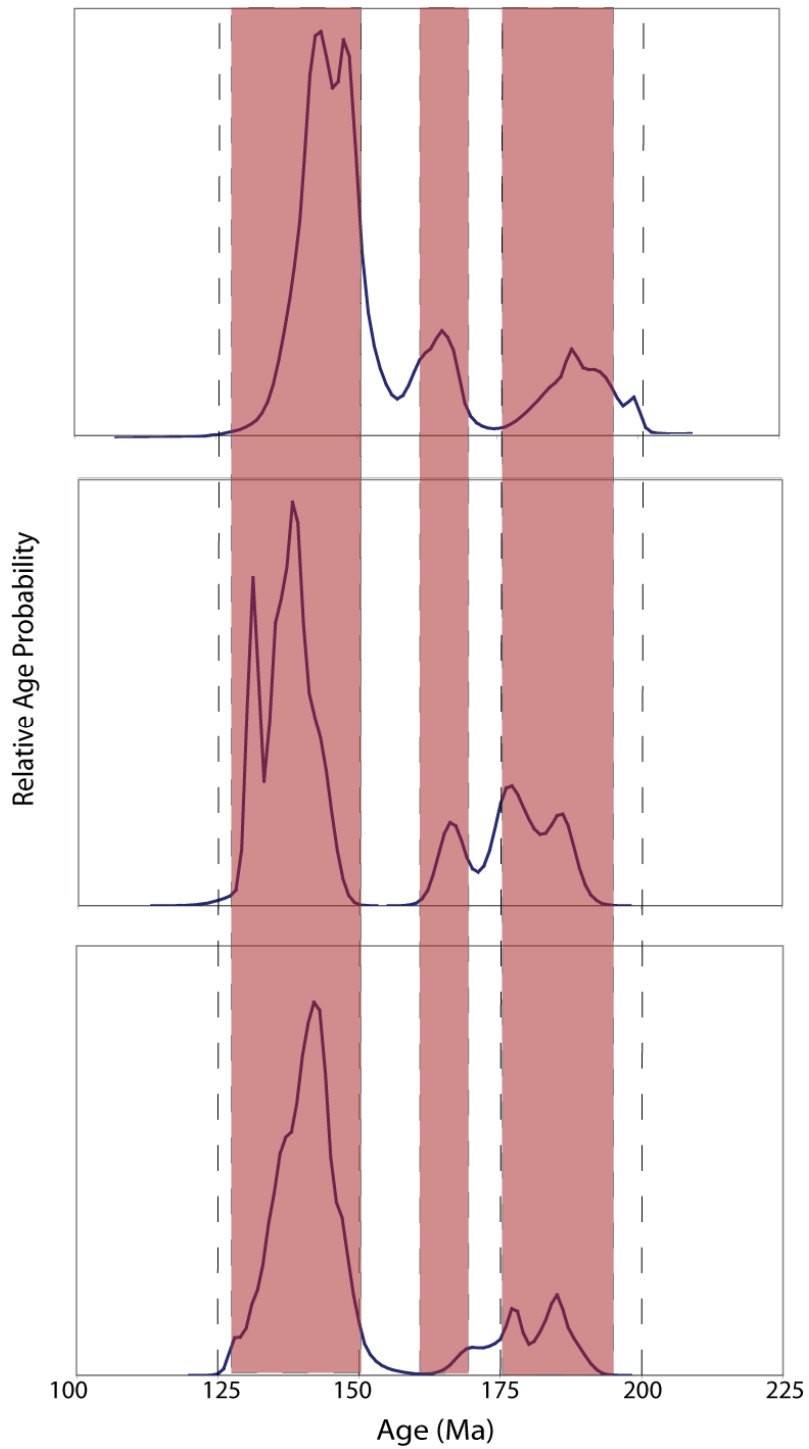


Figure 11. Normalized detrital zircon age graphs with common peak ages highlighted in red. Normalized graphs permit comparison of data from samples with different numbers of grains.

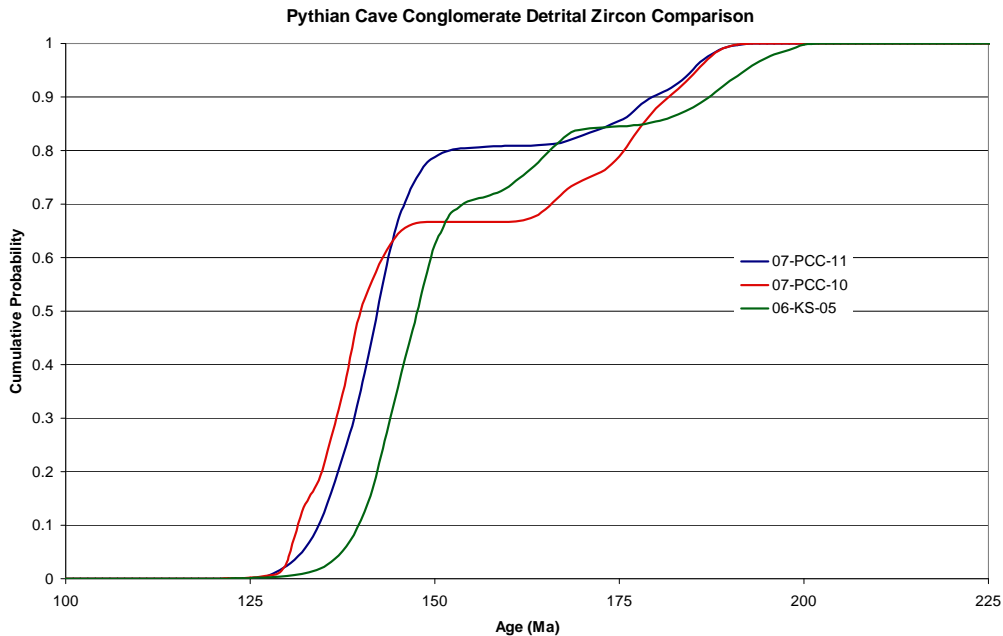


Figure 12. Cumulative probability curves; steep slopes indicate a concentration of ages from ~130-150 Ma, while areas of horizontal slope indicate absent zircon grains of that age, ~150-165 Ma, and prior to 200 Ma.

All four igneous samples provide the same age (within error) of approximately 187-188 Ma (Fig. 13). PCC-04, a felsic volcanic cobble, gave an age of 187.4 +/- 4.2 Ma. PCC-24, one of three granite cobbles tested, produced an age of 187.4 +/- 3.6 Ma. PCC-25, granite, gave 187.5 +/- 3.6 Ma. PCC-26, another granite, gave an age of 188.3 +/- 4.5 Ma. There was no correlation between the age of grains and uranium concentration, suggesting no significant age resetting from crystal lattice damage leading to parent/daughter isotope escape (Fig. 14). The 187-188 Ma igneous age falls within the second oldest and second largest age peak in the sandstone samples (Fig. 11).

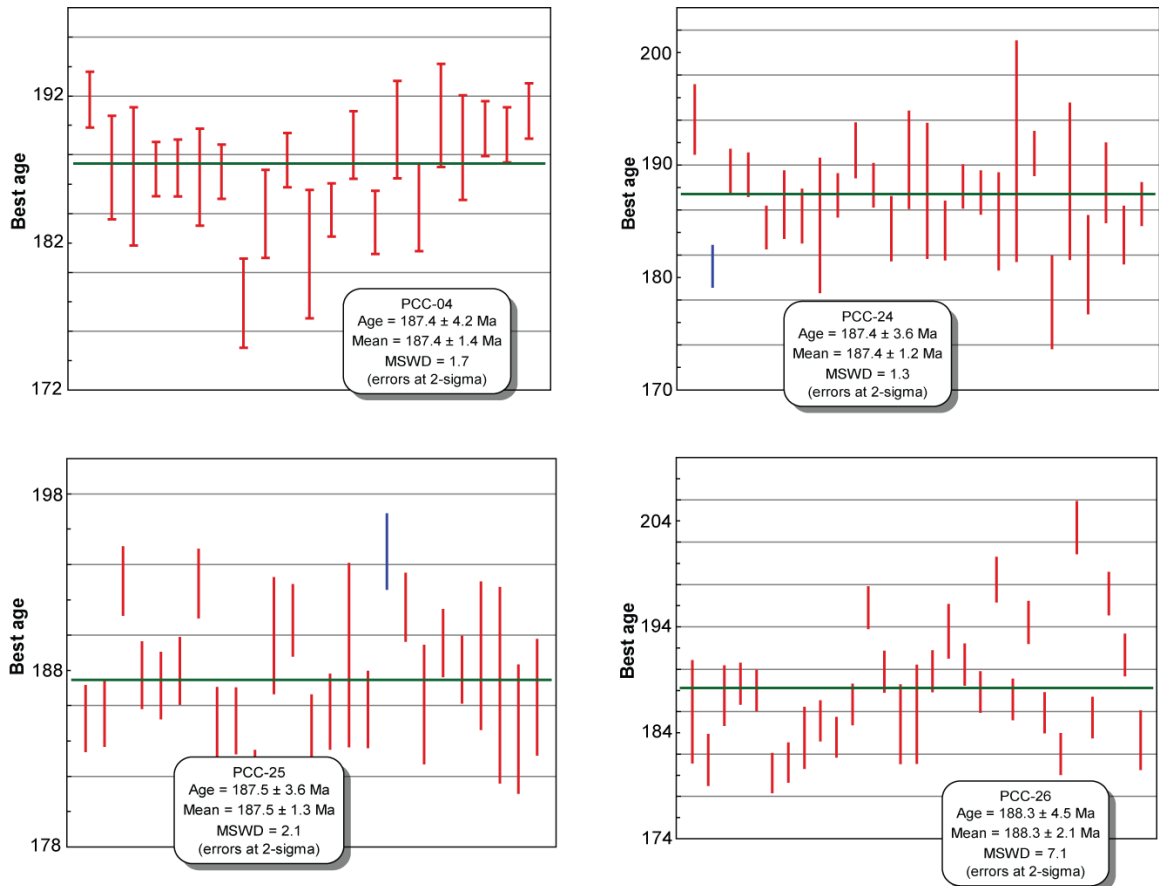
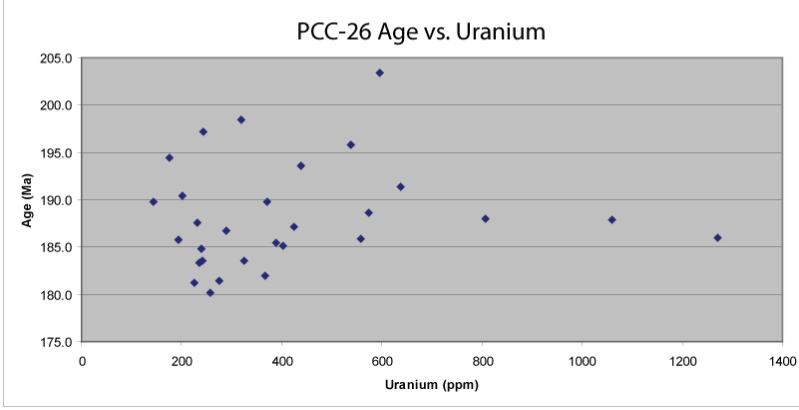
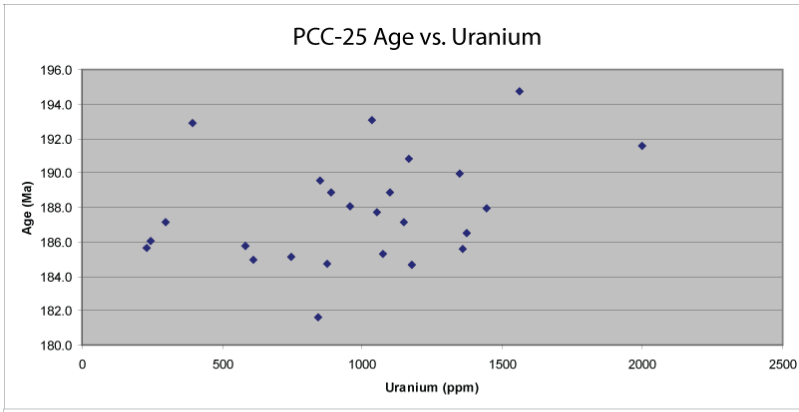
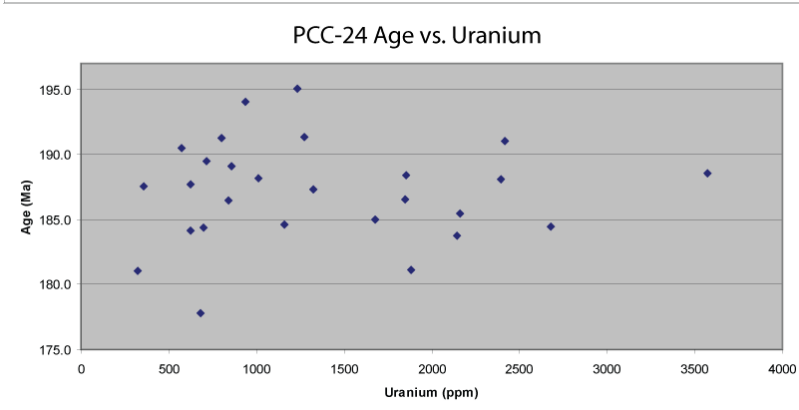
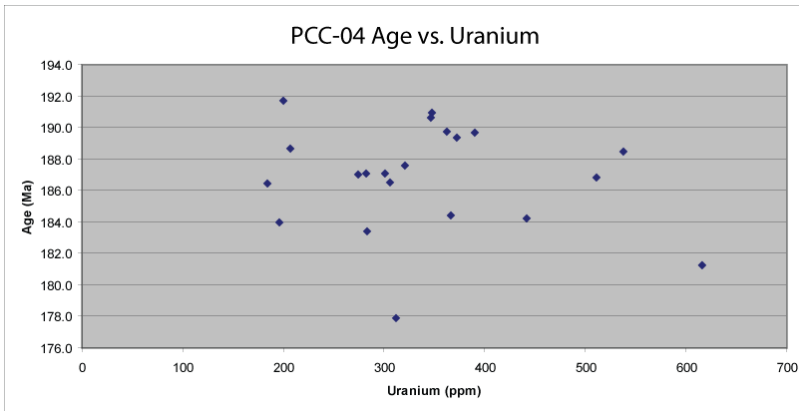


Figure 13. Best fit ages for zircon from four individual cobble clasts. Length of red lines accounts for potential error of each zircon crystal while green line highlights best age without factoring in error. X-axis is individual zircon grains from each cobble sample.



Geochemistry

Geochemistry provides another avenue for analyzing and interpreting provenance for the PCC. Major element data help determine the composition of the source, while trace elements are more useful in characterizing the magmatic history of the source (Rollinson, 1993). Rare Earth Elements (REE) are particularly useful trace elements, as they are the least soluble and therefore least vulnerable to hydrothermal alteration (Rollinson, 1993), which is intense in the PCC volcanic clasts.

Classifying the rock type of the clasts of the PCC based on chemistry is equally effective as classification using traditional, mineral composition analysis (Rollinson, 1993). The total alkalis-silica (TAS) diagram is a commonly-used method for interpreting composition using geochemistry (Rollinson, 1993). The PCC ranges from approximately 60-75% (by weight) silica, with alkali generally below 6% (by weight). These values plot in the andesite-dacite range on the diagram (Fig. 15).

Trace element diagrams are also useful in determining provenance information based on geochemistry of the clasts using multi-element diagrams (Rollinson, 1993). Two different diagrams are used in igneous trace element geochemistry analysis, comparing the rock chemistry with a 'mantle source,' and with 'the most abundant volcanic rock' (Rollinson, 1993). Plotting these graphs indicates the PCC source originated in the lower continental crust (Fig. 16)

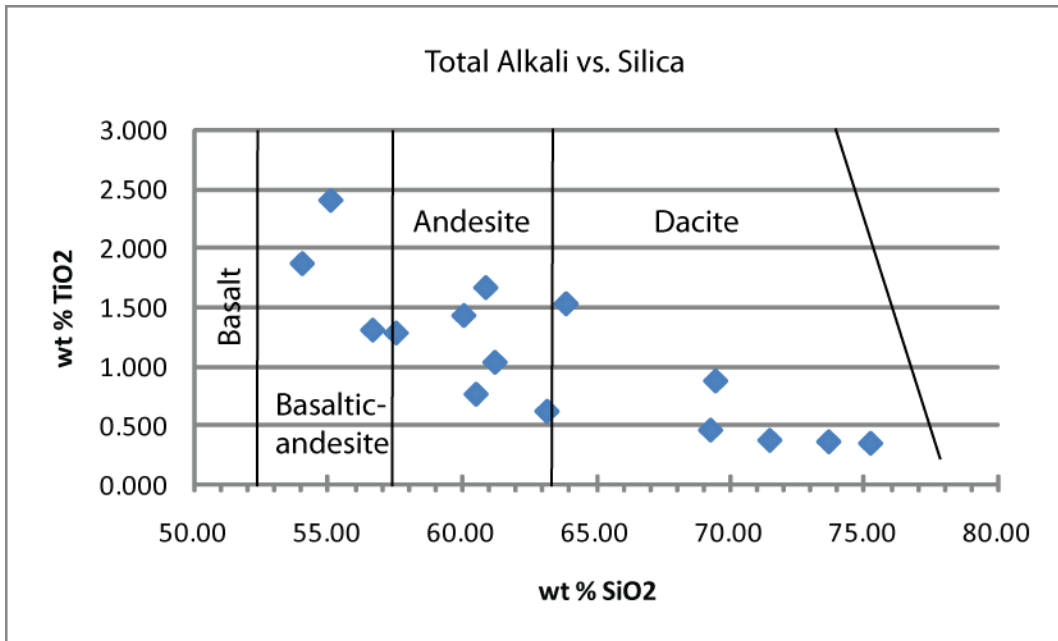


Figure 15. Major element geochemistry plotting total alkali vs. silica. Chemical classification and nomenclature for volcanic rocks by Le Maitre et al. (1989). Data indicate a largely Andesite-Dacite composition for the source of the PCC.

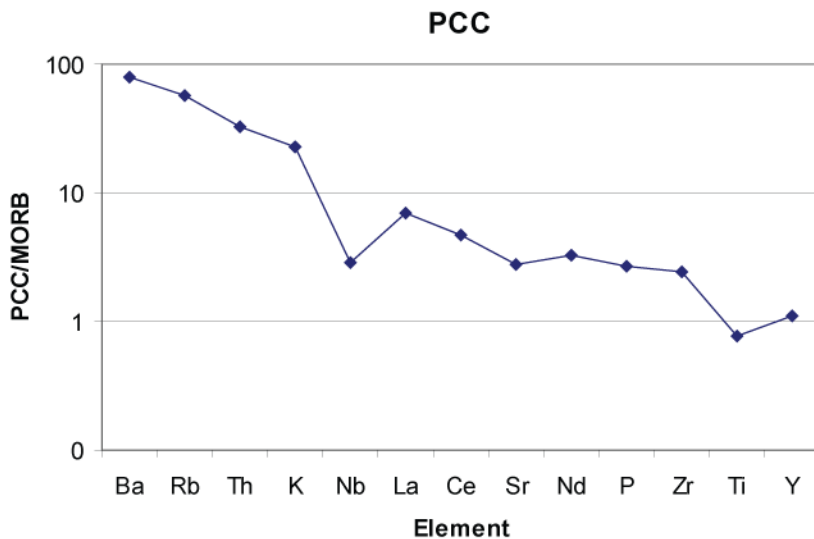


Figure 16. Multi-Element diagram normalized against composition MORB. Spider diagram after Rollinson (1993) aimed at distinguishing magma origin in the crust. Element trends, specifically the Nb and Th anomalies, suggest the PCC had a source with a Lower Continental Crust magma signature.

DISCUSSION

Cobble size data, sandstone textural and compositional immaturity, and depositional environment analysis in previous studies of the PCC (Jameossanaie et al., 1993) all suggest a nearby source for the PCC. Paleoflow direction determined by cobble imbrication and sandstone cross-bed readings in the PCC outcrop suggest an E to NE source (Fig. 4). Clast composition and sandstone point counts indicate that the source was dominated by a volcanic arc (Figs. 5 and 7). Porphyritic volcanic rocks represent a majority in clast counts from multiple studies, and QFL diagrams using sandstone framework grain compositions plot in the dissected arc region (Dickinson, 1983). Quartzite clasts are absent in clast counts, which is significant, because the Antelope Mountain Quartzite is present in most Klamath Mountain-sourced sedimentary deposits on or near the Eastern Klamath terranes, such as the basal unit of the Hornbrook. Sandstone petrography revealed immature texture dominated by angular grains, as well as immature composition, with high percentages of micas (Fig. 8). Accordingly, sandstone petrography results support a proximal, intermediate to felsic source.

Geochemical data support a volcanic arc source with an andesite to dacite composition (Fig. 16). REE values for the PCC suggest a lower continental crustal source, consistent with provenance in the Sierra Nevadan magmatic arc, based on the interpretation made by Bateman et al. (1963) that the Sierra Nevada batholith formed from a lower crustal magma.

The main source of zircon is in felsic to intermediate plutonic rocks (e.g., Poldervaart, 1956; Watson, 1979). Therefore, in attempting to find a source for the PCC zircon, focus is on finding plutonic rocks that match the age signatures of the PCC zircon

grains. Zircon data are used to characterize potential sources by matching the zircon age peaks with the ages of plutonic rocks in a potential source. Age gaps in zircon data are also important, providing information that can be used to exclude potential sources.

Looking first at the underlying Klamath Mountains, several matching age peaks between the PCC and the Klamath Mountains are present. Middle Jurassic plutonism in the Klamath Mountains matches several age peaks in the PCC. However, younger, late Jurassic to early Cretaceous plutonism in the Klamaths trends northwest from the PCC (Hacker et al., 1995), problematic for the SW to W paleoflow readings in the PCC. Compensating for potential rotation of the northern Cordillera terranes would restore a maximum of approximately 40° clockwise rotation, which would result in a new south-directed paleoflow. A northerly source still places the source out of the Klamath terranes based on paleoflow. Within the Klamath terranes, the most closely linked ages to those in the PCC are south of the PCC outcrop, such as the Shasta Bally terrane, excluding the Klamath Mountains as a source. Additionally, if the Klamath Mountains were the source for the PCC, early Cambrian zircon ages and quartzite clasts would be expected, as seen in the basal Hornbrook Formation (Beverly, 2008).

Wyld and others (2006) reconstructed the paleogeography of the Cordilleran terranes back to 100 Ma, the mid-Cretaceous. Their reconstruction suggests that the Klamaths, and hence the PCC, moved north 400 km to their modern position relative to the craton by 110 Ma. Albian deposition of the PCC, as suggested by Jameossanaie and Lindsley-Griffin (1993) and supported by detrital zircon ages, has the PCC deposited after the terrane had been transported north 400 km along strike-slip faults. Thus, this northern placement of the PCC, coupled with the E to NE source direction from

paleoflow data, indicates a northern continuation (now buried or removed) of the Sierra Nevada Mountains as a potential source. Alternatively, the PCC may have been slightly south of its current location, adjacent to the northern Sierra Nevadas. However, if the PCC was deposited much further south relative the Sierra Nevada plutonism, then younger, Early Cretaceous (Aptian-Albian) grains would be expected in the zircon ages. Northern deposition of the PCC supports Jurassic to Early Cretaceous zircon ages (minimum age of Valanginian), expected from the older plutonism trending northwest in the Sierra Nevada batholiths. This interpretation would support Wyld and others' (2006) paleogeography reconstruction, which requires a now-buried or eroded northern continuation of the Sierran terranes and magmatic arc as the source for the PCC.

CONCLUSIONS

The source of the PCC was to the N-NE relative to the PCC at the time of deposition, based on paleoflow directions measured from cobble imbrication. Sandstone petrography, sandstone composition and cobble composition indicate a volcanic arc source for the PCC. The PCC was located close to the source at the time of deposition, as indicated by cobble size and sandstone textural and compositional immaturity. Zircon age data support Albian deposition, confirming interpretation derived from palynomorphs (Jameossanaie and Lindsley-Griffin, 1993). The source for the PCC must have contained plutonic ages no older than 200 Ma exposed during deposition, with peaks at approximately 195-175 Ma, 165-170 Ma and 130-150 Ma; the source will have corresponding age gaps in plutonism as well. Additionally, zircon data indicate a maximum depositional age of approximately 131 Ma observed from the oldest detrital zircon age peak. The PCC, and therefore the Klamath Mountains as well, must have

moved north of the younger, southern Sierra Nevadas by time of deposition, probably by 108 Ma, as reconstructed by Wyld et al (2006). The PCC had moved north, adjacent to the northern Sierra Nevadas or a now-buried continuation of the northern Sierras. These results suggest little to no translation of the Klamath Mountains terrane since Cretaceous time, supporting previous paleomagnetism studies by Mankinen and Irwin (1990), along with paleogeographic reconstructions by Ingersoll (1983) and Wyld et al. (2006). Therefore, the PCC provides valuable information about the paleogeography of the northern Cordilleran terranes during Cretaceous time.

ACKNOWLEDGEMENTS

Special thanks to all those who helped fund this project including: Trinity University Summer Undergraduate Research Fellowship, ACS-PRF (through Dr. Kathleen Surpless), Cordilleran Section Student Travel Grant, and Trinity University Herndon Scholarship Funds. Thank you to Dr. George Gehrels and Dr. Victor Valencia for your help and hospitality at the Laser-Chron Center at the University of Arizona. Also, thank you to my advisor, Dr. Kathleen Surpless, and my colleague and field partner, Emily Beverly, for the support during the last year.

REFERENCES

- Bateman, P.C. (1983) A summary of the critical relations in the central part of the Sierra Nevada Batholith, California, U.S.A. Geological Society of America Memoir No. 159, p. 241 – 252.
- Bateman, P.C., L.K. Clark, N.K. Huber, J.G. Moore and C.D. Rinehart (1963) The Sierra Nevada batholith – A synthesis of recent work across the central part. U.S. Geological Survey Professional Paper 414-D. 46p.
- Beverly, E., Surpless, K., Augsburger, G.A., 2008, Provenance Analysis of the Cretaceous Hornbrook Formation of Northern California and Southern Oregon: Evidence for a Non-Klamath Cretaceous Arc Source, Geological Society of America *Abstracts with Programs*, Vol. 40, No. 1, p. 55.
- Burchfiel, B.C., Cowan, D.S., and Davis, G.A., 1992, Tectonic overview of the Cordilleran orogen in the western United States, in Burchfiel, B.C., Lipman, P.W. and Zoback, M.L., eds., *The Geology of North America: The Cordilleran Orogen: Conterminous U.S.* Boulder, Colorado, The Geological Society of America, p. 407-479.
- Cowan, D.S., and Bruhn, R.L., 1992, Late Jurassic to early Late Cretaceous geology of the U.S. Cordillera, in Burchfiel, B.C., Lipman, P.W., and Zoback, M.L., eds., *The Cordilleran Orogen: Conterminous U.S.: Boulder, Colorado*, Geological Society of America, *The Geology of North America*, v. G-3.
- Dickinson, W.R., Beard, S.L., Brakenridge, G.R., Erjavec, J.L., Ferguson, R.C., Inman, K.F., Knepp, R.A., Lindberg, F.A., and Ryberg, P.T., 1983, Provenance of North American Phanerozoic sandstones in relation to tectonic setting: Geological Society of America Bulletin, v. 94, p. 222-235.
- Engelbreton, D.C., Cox, A., and Gordon, R., 1985, Relative motions between oceanic plates and continental plates in the Pacific basin. Geological Society of America, Special Paper 208, 59p.
- Evernden, J.F., and R.W. Kistler (1970) Chronology and Emplacement of Mesozoic Batholithic complexes in California and Western Nevada. U.S. Geological Survey Professional Paper 623, 42p.
- Gehrels, G.E., and Juiz, J., 2007, U-Th-Pb geochronology of zircon by Laser-Ablation Multicollector ICP Mass Spectrometry at the Arizona LaserChron Center: *Journal of Analytical Atomic Spectrometry*.
- Griffin, J.R., Lindsley-Griffin, N., Wtzstein, E.E., and Jameossanaie, A., 1993, Post-Accretion History and Paleogeography of a Cretaceous Overlap Sequence in Northern California, in Dunn, G., and McDougall, K., eds., 1993, *Mesozoic Paleogeography of the Western United States-II: Pacific Section SEPM*, Book 71, p. 99-112.
- Hacker, B.R., Donato, M.M., Barnes, C.G., McWilliams, M.O., and Ernst, W.G., 1995, Timescales of orogeny: Jurassic construction of the Klamath Mountains, *Tectonics*, vol. 14, no. 3, p. 677-703.
- Hacker, B.R., and Ernst, W.G., 1993, Jurassic Orogeny in the Klamath Mountains: A Geochronological Analysis: *Mesozoic Paleogeography of the Western United States-II*, v. Book 71, p. 37-60.

- Harper, G.D., Saleeby, J.B., and Heizler, M., 1994, Formation and emplacement of the Josephine ophiolite and the Nevadan orogeny in the Klamath Mountains, California-Oregon: U/Pb zircon and $^{40}\text{Ar}/^{39}\text{Ar}$ geochronology, *J. Geophys. Res.*, 99, 4293-4321.
- Harper, G.D., and Wright, J.E., 1984, Middle to Late Jurassic tectonic evolution of the Klamath Mountains, California-Oregon, *Tectonics*, 3, 759-772.
- Harwood, D.S., 1983, Tectonism and metamorphism in the northern Sierra terrane, northern California, *in* Ernest, W.G., ed., *Metamorphism and crustal evolution of the western United States; Rubey Volume 7: Englewood Cliffs, New Jersey, Prentice-Hall*, p. 764-788.
- Hotz, P.E., 1977, *Geology of the Yreka quadrangle, Siskiyou County, California: U.S. Geological Survey Bulletin 1436*, 72 p.
- Ingersoll, R.V., 1983, Petrofacies and Provenance of Late Mesozoic Forarc Basin, Northern and Central California: *The American Association of Petroleum Geologists Bulletin*, v. 67, p. 1125--1142.
- Irving, E., Woodsworth, G.J., Wynne, P.J., and Morrison, A., 1985, Paleomagnetic evidence for displacement from the south of the Coast plutonic complex, British Columbia: *Canadian Journal of Earth Sciences*, v. 22, p. 584-598.
- Irwin, W.P., Wooden, J.L., 1999, *Plutons and accretionary episodes of the Klamath Mountains, California and Oregon: U.S. Geological Survey Open-File Report*.
- Jameossanaie, A., Lindsley-Griffin, N., 1993, Palynology and Plate Tectonics – A Case Study on Cretaceous Terrestrial Sediments in the Eastern Klamath Mountains of Northern California, U.S.A., *Palynology*, 17: 11-45.
- Le Maitre, R.W., Bateman, P., Dudek, A., Keller, J., Lameyre, J., Le Bas, M.J., Sabine, P.A., Schmid, R., Sorensen, H., Streckeisen, A., Woolley, A.R., and Zanettin, B., 1989, *A Classification of Igneous Rocks and Glossary of Terms: Recommendations of the International Union of Geological Sciences Subcommission on the Systematics of Igneous Rocks*. Oxford: Blackwell Scientific.
- Mankinen, E.A., and Irwin, W.P., 1990, Review of paleomagnetic data from the Klamath Mountains, Blue Mountains and Sierra Nevada: Implications for paleogeographic reconstructions, *in* Harwood, D.S., and Miller, M.M., eds., *Paleozoic and early Mesozoic paleogeographic relations; Sierra Nevada, Klamath Mountains, and related terranes: Boulder, Colorado, Geological Society of America Special Paper 255*, p. 397-407.
- Miller, D.M., Nilsen, T.H., and Bilodeau, W.L., 1992, Late Cretaceous to early Eocene geologic evolution of the U.S. Cordillera, *in* Burchfiel, B.C., Lipman, P.W., and Zoback, M.L., eds., *The Cordilleran Orogen: Conterminous U.S.: Boulder, Colorado, Geological Society of America, The Geology of North America*, v. G-3.
- Nilsen, T.H., 1993, *Stratigraphy of the Cretaceous Hornbrook Formation, Southern Oregon and Northern California, U.S. Geological Survey Professional Paper 1521: United States Government Printing Office, Washington*.
- Poldervaart, A., 1956, Zircons in Rocks II., *Igneous Rocks, American Journal of Science*, 254, 521-554.

- Potter, A.W., Boucot, A.J., Bergstrom, S.M., Blodgett, R.B., Dean, W.T., Flory, R.A., Ormiston, A.R., Pedder, A.E.H., Rigby, J.K., Rohr, D.M., and Savage, N.M., 1990, Early Paleozoic stratigraphic, paleogeographic, and biogeographic relations of the eastern Klamath belt, northern California, in Harwood, D.S. and Miller, M.M., eds., Paleozoic and early Mesozoic paleogeographic relations; Sierra Nevada, Klamath Mountains, and related terranes: Boulder, Colorado, Geological Society of America Special Paper 255, p. 57-73.
- Rollinson, H., 1993, Using Geochemical Data: Evaluation, Presentation, Interpretation, Longman Geochemistry Series: London, Prentice Hall, 352 p.
- Rubin, C.M., Miller, M.M., and Smith, G.M., 1990, Tectonic development of Cordilleran mid-Paleozoic volcano-plutonic complexes; Evidence for convergent margin tectonism, in Harwood, D.S. and Miller, M.M., eds., Paleozoic and early Mesozoic paleogeographic relations; Sierra Nevada, Klamath Mountains, and related terranes: Boulder, Colorado, Geological Society of America Special Paper 255, p. 1-15.
- Schweickert, R.A., Bogen, N.L., Girty, G.H., Hanson, R.E., and Merguerian, C., 1984, Timing and structural expression of the Nevadan orogeny, Sierra Nevada, California, Geological Society of America Bulletin, 95, 967-979.
- Snoke, A.W., and Barnes, C.G., 2006, The development of tectonic concepts for the Klamath Mountains province, California and Oregon, in Snoke, A.W. and Barnes, C.G., eds., Geological studies in the Klamath Mountains province, California and Oregon: A volume in honor of William P. Irwin: Boulder, Colorado, Geological Society of America Special Paper 410, p. 1-29.
- Stern, T.W., P.C. Bateman, B.A. Morgan, M.F. Newell, and D.L. Peck (1981) Isotopic U-Pb ages of zircon from the granitoids of the central Sierra Nevada, California. U.S. Geological Survey Professional Paper 1185, 17p.
- Stock, J., and Molnar, P., 1988, Uncertainties and implications of the Late Cretaceous and Tertiary position of North America relative to the Farallon, Kula, and Pacific plates: Tectonics, v. 7, p. 1339-1348.
- Watson, E.B., 1979, Zircon saturation in felsic liquids: experimental data and applications to trace element geochemistry. *Contrib. Mineral. Petrol.* **70**, 407-419.
- Wells, R.E., Jayko, A.S., Niem, A.R., Black, G., Wiley, T., Baldwin, E., Molenaar, K.M., Wheeler, K.L., DuRoss, C.B., Givler, R.W., 2000, Geologic Map and Database of the Roseburg 30 X 60' Quadrangle, Douglas and Coos Counties, Oregon: U.S. Geological Survey Open File Report 00-376.
- Wetzstein, E.E., 1986, Sedimentology and tectonic significance of a Cretaceous conglomerate in the eastern Klamath Mountains, California, Master's Thesis: Lincoln, Nebraska: 53 p.
- Wyld, S.J., Umhoefer, P.J., and Wright, J.E., 2006, Reconstructing northern Cordilleran terranes along known Cretaceous and Cenozoic strike-slip faults: Implications for the Baja British Columbia hypothesis and other models, in Haggart, J.W., Enkin, R.J. and Monger, J.W.H., eds., Paleogeography of the North American Cordillera: Evidence For and Against Large-Scale Displacements: Geological Association of Canada Special Paper 46, p. 277-298.

APPENDIX

GEOCHEMISTRY TABLES

Date	SUR 07 PCC-01 16-Oct- 07	SUR 07 PCC-02 16-Oct- 07	SUR 07 PCC-03 16-Oct- 07	SUR 07 PCC-05 16-Oct- 07	SUR 07 PCC-06 16-Oct- 07	SUR 07 PCC-07 16-Oct- 07	SUR 07 PCC-08 16-Oct- 07
------	-----------------------------------	-----------------------------------	-----------------------------------	-----------------------------------	-----------------------------------	-----------------------------------	-----------------------------------

Unnormalized Major Elements (Weight %):

SiO2	58.88	61.41	55.59	61.27	70.03	72.50	58.32
TiO2	1.609	1.467	1.234	0.593	0.357	0.347	0.729
Al2O3	12.75	12.29	16.25	17.20	14.51	13.49	17.09
FeO*	9.93	9.61	7.43	5.44	2.48	2.49	5.73
MnO	0.130	0.193	0.175	0.126	0.072	0.035	0.257
MgO	2.36	2.33	2.61	2.12	0.62	0.74	2.44
CaO	3.38	2.51	6.13	3.48	1.89	0.86	4.95
Na2O	3.44	1.88	3.76	4.84	4.13	5.57	4.73
K2O	3.63	4.06	2.93	1.75	3.85	2.38	1.92
P2O5	0.617	0.404	0.515	0.210	0.086	0.050	0.234
Sum	96.74	96.17	96.63	97.04	98.02	98.45	96.39

Normalized Major Elements (Weight %):

SiO2	60.87	63.86	57.53	63.15	71.44	73.64	60.50
TiO2	1.663	1.525	1.277	0.611	0.364	0.352	0.756
Al2O3	13.18	12.78	16.82	17.73	14.80	13.70	17.73
FeO*	10.26	9.99	7.69	5.60	2.53	2.53	5.95
MnO	0.135	0.201	0.181	0.130	0.074	0.036	0.267
MgO	2.44	2.43	2.70	2.18	0.64	0.75	2.53
CaO	3.50	2.61	6.35	3.59	1.93	0.87	5.13
Na2O	3.56	1.96	3.89	4.99	4.21	5.65	4.90
K2O	3.75	4.22	3.03	1.80	3.93	2.42	1.99
P2O5	0.638	0.420	0.533	0.216	0.088	0.050	0.243
Total	100.00	100.00	100.00	100.00	100.00	100.00	100.00

Unnormalized Trace Elements (ppm):

Ni	8	10	13	4	8	4	19
Cr	2	12	24	5	4	3	6
Sc	27	25	21	9	5	9	15
V	120	211	168	92	32	21	104
Ba	1517	1722	590	733	985	1705	1053
Rb	70	112	85	49	106	55	45
Sr	99	282	404	451	178	196	491
Zr	306	180	301	106	188	229	84
Y	64	36	41	17	17	38	22
Nb	11.2	7.0	13.8	6.3	7.3	4.5	2.3
Ga	18	14	17	19	15	13	18
Cu	47	94	34	82	12	4	28
Zn	33	78	70	73	46	44	385
Pb	2	7	7	4	10	7	12
La	28	20	29	18	14	15	14
Ce	71	44	69	32	29	38	33
Th	8	4	11	2	12	8	1
Nd	42	26	34	17	12	19	18

	SUR 07 PCC-09	SUR 07 PCC-13	SUR 07 PCC-14	SUR 07 PCC-15	SUR 07 PCC-16	SUR 07 PCC-17	SUR 07 PCC-20	SUR 07 PCC-21
--	------------------	------------------	------------------	------------------	------------------	------------------	------------------	------------------

Date	16-Oct-07	16-Oct-07	16-Oct-07	17-Oct-07	17-Oct-07	17-Oct-07	17-Oct-07	17-Oct-07
------	-----------	-----------	-----------	-----------	-----------	-----------	-----------	-----------

Unnormalized Major Elements (Weight %):

SiO2	67.77	53.55	52.92	58.08	54.81	59.70	73.85	67.63
TiO2	0.848	2.338	1.829	1.379	1.259	1.003	0.333	0.440
Al2O3	12.22	13.30	16.49	14.30	15.25	16.54	13.01	15.76
FeO*	6.05	11.57	10.37	9.58	8.20	6.73	1.97	3.37
MnO	0.144	0.181	0.196	0.217	0.173	0.068	0.039	0.031
MgO	0.71	3.06	3.06	3.11	0.17	1.35	0.23	0.92
CaO	2.68	8.66	8.46	5.54	16.38	3.84	1.61	0.44
Na2O	3.47	3.74	3.14	3.74	0.08	3.86	5.45	6.46
K2O	3.48	0.26	1.00	0.26	0.02	4.03	1.66	2.51
P2O5	0.238	0.536	0.472	0.511	0.393	0.417	0.049	0.118
Sum	97.62	97.19	97.93	96.72	96.75	97.54	98.20	97.67

Normalized Major Elements (Weight %):

SiO2	69.43	55.10	54.03	60.05	56.66	61.21	75.20	69.24
TiO2	0.869	2.405	1.867	1.425	1.301	1.028	0.339	0.451
Al2O3	12.52	13.68	16.84	14.78	15.77	16.96	13.25	16.14
FeO*	6.20	11.91	10.59	9.91	8.48	6.90	2.01	3.45
MnO	0.148	0.186	0.200	0.225	0.179	0.070	0.040	0.032
MgO	0.73	3.15	3.13	3.22	0.18	1.39	0.24	0.94
CaO	2.74	8.91	8.64	5.73	16.93	3.93	1.64	0.45
Na2O	3.56	3.85	3.20	3.86	0.08	3.96	5.55	6.62
K2O	3.57	0.26	1.02	0.27	0.02	4.13	1.69	2.57
P2O5	0.244	0.551	0.482	0.528	0.406	0.427	0.049	0.121
Total	100.00	100.00	100.00	100.00	100.00	100.00	100.00	100.00

Unnormalized Trace Elements (ppm):

Ni	6	17	16	21	1	6	3	8
Cr	4	26	16	16	16	4	2	7
Sc	18	46	33	22	22	15	9	6
V	10	434	326	199	202	67	29	75
Ba	1255	240	782	119	28	1135	1777	712
Rb	90	5	30	5	2	115	26	49
Sr	145	285	302	233	1867	322	173	193
Zr	324	269	224	210	142	323	218	101
Y	68	61	54	45	32	41	39	9
Nb	8.1	6.2	6.0	7.4	5.5	12.8	4.0	3.5
Ga	16	15	20	18	27	19	12	16
Cu	17	106	20	116	3	30	2	10
Zn	34	135	139	184	10	51	24	46
Pb	7	15	3	7	70	3	5	4
La	25	23	18	28	20	32	12	7
Ce	52	50	46	55	44	74	41	17
Th	6	6	3	5	4	12	8	7
Nd	36	34	30	30	26	40	24	8

Date	SUR 07 PCC-01 16-Oct-07	SUR 07 PCC-02 16-Oct-07	SUR 07 PCC-03 16-Oct-07	SUR 07 PCC-05 16-Oct-07	SUR 07 PCC-06 16-Oct-07	SUR 07 PCC-07 16-Oct-07	SUR 07 PCC-08 16-Oct-07
------	-------------------------------	-------------------------------	-------------------------------	-------------------------------	-------------------------------	-------------------------------	-------------------------------

sum tr.	2472.85	2883.53	1931.2	1721.18	1678.65	2410.06	2350.05
in %	0	0	0	0	0	0.24101	0.235
sum m+tr	96.9888	96.4535	96.823	97.2083	98.1836	98.6899	96.623
M+Toxides	97	97	97	97	98	98.7284	96.6673

Date	SUR 07 PCC-09 16-Oct-07	SUR 07 PCC-13 16-Oct-07	SUR 07 PCC-14 16-Oct-07	SUR 07 PCC-15 17-Oct-07	SUR 07 PCC-16 17-Oct-07	SUR 07 PCC-17 17-Oct-07	SUR 07 PCC-20 17-Oct-07	SUR 07 PCC-21 17-Oct-07
	2121	1773	2065	1319	2523	2298.95	2407.54	1276
	0	0	0	0	0	0.22989	0.24075	0
	98	97	98	97	97	97.7679	98.4444	98
	97.8677	97.4158	98.1901	96.8843	97.0578	97.8115	98.4824	98

ZIRCON TABLES

DETRITAL ZIRCON

xx = indicates discordant data

Spot Name	ppm U	ppm Th	238Th /232U	Total 238 /206	% err	Total 207 /206	% err
std	470	84	0.03	0.07	1.0	16.9190	1.0
std	444.11288	119.8389	0.0312142	0.06884	1.28	16.81	1.4
std	475.04252	87.119792	0.0310063	0.06874	1.76	16.612	1.13
std	483.86033	115.5937	0.0306108	0.06998	1	16.654	1.5
std	611.65122	192.15226	0.0251442	0.06837	1	16.755	1.05
P11-1	74.724182	37.606262	0.0050761	0.01697	1.58	24.467	21.88
P11-2	102.6248	56.223018	0.0052091	0.01674	1.55	19.502	11.13
P11-3	106.05769	76.579271	0.006149	0.01687	1.46	21.553	13.19
P11-4	201.42967	122.32389	0.0059345	0.01695	1	21.023	8.34
P11-5	104.45063	73.514443	0.0061134	0.01593	1	19.832	10.49
std	573.01441	122.5931	0.0290656	0.07016	1.13	16.847	2.21
P11-6	108.98574	79.581973	0.0057236	0.01691	1.04	19.894	10.34
P11-7	171.61068	138.84911	0.0069474	0.01616	1.7	20.486	7.62
P11-8	112.06524	71.070864	0.0061201	0.01689	2.09	20.988	8.27
P11-9	256.33903	145.0616	0.0084153	0.02242	1.47	18.883	2.86
P11-10	129.22967	67.281247	0.0058281	0.01655	1.59	19.582	7.35
std	739.40845	158.37703	0.0224039	0.06617	2.19	16.777	1.34
P11-11	931.54913	759.26959	0.0084561	0.02164	1.56	19.489	1.97
P11-12	599.44259	42.348461	0.004274	0.01644	1.81	20.07	3.76
P11-13	152.45214	70.822365	0.0076572	0.0167	1	20.124	8.76
P11-14	108.37993	50.279737	0.0048155	0.01706	1	21.899	8.59
P11-15	552.53489	290.68232	0.009311	0.02018	2.44	19.333	5.74
std	696.49737	157.23808	0.027554	0.06841	1.48	16.926	1.37

P11-16	75.178535	37.399179	0.0069554		0.01674	3.17	19.949	14.31
P11-17	94.951289	68.420203	0.0067046		0.01714	3.42	19.562	9.94
P11-18	455.63157	235.92959	0.0092803		0.02075	2.71	19.811	3.31
P11-19	726.88851	358.00498	0.0089357		0.01993	1.4	20.11	2.48
P11-20	255.32936	187.45148	0.0069351		0.01688	2.92	19.628	7.08
std	574.31857	114.80678	0.0274673		0.0683	1.13	16.792	1
P11-21	188.44697	102.6096	0.0060722		0.0168	1.56	20.402	9.69
P11-22	223.89489	91.282159	0.0098227		0.02216	1.56	19.491	5.58
P11-23	106.03245	64.56846	0.0058666		0.01713	1.58	20.007	15.63
P11-24	200.57987	158.23207	0.0075261		0.01709	1.15	21.012	5.58
P11-25	137.56788	105.90221	0.0067703		0.01682	1.48	17.756	8.42
std	583.95253	129.61321	0.0276969		0.06939	2.04	16.83	1.23
P11-26	93.975272	45.040539	0.0056669		0.01656	2.61	21.179	12.99
P11-27	504.668	324.74746	0.0087615		0.02033	1.91	19.809	4.71
P11-28	398.96369	181.90165	0.008807		0.02193	1.56	19.679	2.75
P11-29	386.26706	192.44217	0.0067725		0.01559	1.05	19.642	2.63
P11-30	179.93206	102.96164	0.0072393		0.01629	3.09	20.03	7.06
std	591.89529	164.36173	0.0262274		0.0687	1.69	16.748	2.47
P11-31	113.20953	44.729915	0.0082806		0.0159	2.39	21.676	13.39
P11-32	232.71269	149.8038	0.0083431		0.01632	1	20.061	6.19
P11-33	120.68953	61.462216	0.0076513		0.01618	1.41	18.667	7.48
P11-34	189.22946	95.051069	0.0072212		0.01544	1.56	20.049	6.89
P11-35	169.53243	69.807659	0.0083456		0.01621	1.66	20.553	7.3
std	487.74757	102.23685	0.0288051		0.0692	1.05	16.708	2.01
P11-36	95.573921	369.74659	0.0078978		0.0171	1	8.652	6.97
P11-37	63.903858	33.361061	0.0074474		0.01758	1.43	20.081	16.09
P11-38	65.485679	40.671089	0.0082719		0.01709	2.16	22.342	30.96
xx	49.112156	24.663578	0.0078195		0.01729	4.7	28.957	30.51
P11-40	69.16257	36.819346	0.0066664		0.01737	1	19.743	12.15
std	406.83914	63.96792	0.033086		0.06991	1.4	16.746	3.16
P11-41	161.12691	95.485943	0.0081875		0.01579	1	19.272	7.14
P11-42	182.76756	102.8581	0.0085856		0.0163	1.53	20.819	3.93
P11-43	260.13372	126.63122	0.0109711		0.02097	1	19.907	3.9
P11-44	82.372452	35.825348	0.0066136		0.0166	1.49	19.153	19.22
P11-45	42.633423	15.469096	0.006393		0.01649	2.36	22.38	27.3
std	467.6635	74.653399	0.0277698		0.06698	1.61	16.704	1.67
P11-46	59.881996	30.213401	0.0074763		0.01671	1.45	17.363	13.2
P11-47	128.49766	59.287845	0.0064604		0.01583	1.13	20.557	7.49
P11-48	53.150846	24.539328	0.0062441		0.01612	1.53	19.951	15.37
xx	247.05004	705.82149	0.009071		0.01712	1	12.098	5.92
P11-50	71.560542	41.789337	0.0073453		0.01672	1.41	21.034	17.75
std	476.19523	111.28637	0.0274021		0.06784	1.14	16.704	1.41
P11-51	745.81146	86.809168	0.0122305		0.02185	1.07	19.885	2.59
P11-52	85.233191	33.091854	0.007821		0.01646	1.83	16.421	11.22
xx	50.820185	19.859254	0.0060743		0.01636	2.8	25.418	32.32
P11-54	150.94605	77.449019	0.0079985		0.01662	2.71	20.181	5.99
xx	380.63814	86.974834	0.011538		0.02254	1	19.503	4.02
std	511.71046	76.206521	0.0279167		0.06812	1	16.856	2.86

P11-56	211.81247	123.75276	0.0081877		0.01629	2.3	20.984	5.35
P11-57	96.095585	58.003931	0.0079835		0.01702	1.42	20.35	12.35
P11-58	74.000584	31.849356	0.0074983		0.01624	1.91	18.526	13.83
P11-59	53.302297	18.016216	0.0084291		0.01718	1	18.479	26.68
P11-60	109.60837	43.073251	0.0083556		0.01563	2.44	20.765	7.89
std	485.61884	87.181917	0.0273418		0.06898	1.61	16.935	1.99
P11-61	121.80858	82.750342	0.009022		0.01737	2.79	18.255	8.6
xx	93.184362	257.34197	0.0092676		0.01697	2.3	9.605	5.82
P11-63	68.615664	28.701695	0.007399		0.01711	1.92	21.354	13.11
P11-64	99.326537	38.60026	0.0078569		0.01653	1.45	21.499	14.93
P11-65	119.36012	61.234425	0.0079049		0.01674	1.6	19.941	13.26
std	419.5526	87.285459	0.0279733		0.06891	1.28	16.663	3.12
P11-66	162.19548	103.74855	0.0089799		0.01751	2.12	20.522	7.75
P11-67	103.82799	40.774631	0.007963		0.01654	1.6	23.031	14.22
P11-68	152.14924	78.795058	0.0107397		0.02106	1.13	19.033	5.18
P11-69	86.730872	41.540837	0.007499		0.01618	1.18	21.194	16.63
P11-70	70.517214	27.894072	0.007637		0.01749	1	21.558	14.95
std	489.19476	95.589484	0.0271874		0.06943	1	16.945	1.23
P11-71	116.99581	44.087958	0.0074021		0.01669	3.38	21.366	11.09
P11-72	189.89416	29.385069	0.0076862		0.01814	3.24	18.511	6.68
xx	66.571077	31.68369	0.0069381		0.01768	2.92	23.304	34.14
xx	112.80567	32.988312	0.011492		0.02402	1	19.376	8.86
xx	81.404849	37.067846	0.0069535		0.01646	3.91	12.297	22.21
std	440.94924	112.3632	0.0297		0.06903	1.06	16.798	3.24
P11-76	90.029136	38.434593	0.0076983		0.01648	1.4	19.417	13.76
P11-77	204.31565	74.052859	0.0106305		0.02174	2.51	19.657	4.68
P11-78	140.98394	101.57418	0.00704		0.01665	1.23	18.386	5.76
P11-79	137.87079	101.34639	0.005665		0.01711	1.22	20.333	6.27
P11-80	98.274795	46.842161	0.0047748		0.01628	1	21.981	10.53
std	494.647	91.15791	0.0272336		0.0689	1	16.76	2.36
P11-81	104.88815	45.744621	0.0045742		0.01572	1	23.568	18.45
P11-82	84.745183	41.02313	0.0053242		0.01608	2.04	19.897	9.79
P11-83	72.09062	38.331052	0.0067913		0.01711	2.23	18.153	6.26
P11-84	91.737165	65.396792	0.0051839		0.01755	1.17	21.517	17.05
P11-85	188.2871	96.562774	0.0054935		0.01671	1.3	21.241	6.68
std	450.56637	132.71946	0.0289148		0.06961	1	16.591	2.07
P11-86	151.88841	67.840371	0.005047		0.01683	2.6	20.713	9.12
P11-87	75.430953	45.786038	0.0039494		0.0169	1.53	24.512	11.15
P11-88	630.47319	267.71682	0.0061756		0.01708	1.22	15.697	4.26
P11-89	191.1226	93.352989	0.0073105		0.02224	1.39	19.594	9.43
xx	405.84629	322.92513	0.0066934		0.01759	1.22	13.946	4.18
std	703.16962	157.3002	0.0225873		0.06838	2.05	16.799	1.19
P11-91	163.7773	143.11502	0.0059697		0.01688	2.37	20.752	5.83
P11-92	491.7526	306.23425	0.0077769		0.02102	1.43	19.599	3.88
P11-93	179.98255	85.173213	0.0076717		0.0223	2.03	19.547	4.94
P11-94	223.32274	114.3512	0.0079549		0.02179	2.15	19.705	3.72
xx	97.180983	56.720017	0.0068872		0.01663	3.9	13.612	32.72
std	510.4063	134.37612	0.0290802		0.07033	1	16.848	1.58

P11-96	153.71423	85.960128	0.0057172		0.01533	1.16	21.716	12.57
P11-97	422.6321	187.80352	0.0076426		0.02123	2.04	19.423	3.53
P11-98	81.968583	36.591555	0.005138		0.01809	1.36	21.537	17.79
P11-99	97.862512	56.160893	0.0049632		0.01721	1.85	21.889	7.8
P11-100	109.64202	90.971535	0.0061413		0.01792	1	21.668	10.3
std	576.85117	138.41424	0.0266182		0.07032	1	16.816	1.2
P10-1	332.85538	410.50051	0.0059086		0.01662	1	19.479	3.37
P10-2	271.00453	242.16279	0.0063559		0.01679	2.27	19.815	5.44
P10-3	201.64002	183.24769	0.0041719		0.01635	1.82	19.59	4.71
P10-4	98.005549	40.04984	0.0062562		0.02118	1.77	19.01	6.71
P10-5	188.19455	141.18915	0.005117		0.01585	1.45	20.331	9.05
std	502.56451	118.30648	0.0299032		0.0679	1.77	16.853	1.08
xx	287.4117	707.16753	0.0069092		0.02128	1.36	11.043	4.98
xx	263.87792	1338.1285	0.004433		0.01649	2.95	10.455	8.28
xx	658.53368	423.79523	0.006774		0.0169	1.26	14.638	2.2
xx	287.1677	593.08554	0.0052781		0.0173	1	11.693	1.22
P10-10	1.3882998	3.6860763	0.2591902		0.64719	6.74	1.188	4.09
std	645.84546	233.87947	0.0234448		0.06986	1.15	16.806	1
P10-11	206.56218	91.282159	0.0072508		0.02124	1.7	18.793	3.08
P10-12	176.78525	142.88723	0.0066587		0.01629	1	19.457	8.27
P10-13	148.72477	83.827173	0.0088903		0.02245	1.68	20.256	6.02
P10-14	182.09444	194.98929	0.0053012		0.01655	1.88	20.481	7.66
P10-15	177.76127	98.095188	0.0045018		0.01586	1	19.877	8.82
std	434.80707	76.372188	0.0290441		0.06979	1.23	16.883	1.83
P10-16	338.30762	299.1313	0.0050882		0.01646	1.84	19.754	3.74
P10-17	26.865704	6.7301955	1.7254968		0.65701	4.55	1.214	2.15
P10-18	121.15229	635.04054	0.0041943		0.01758	2.58	7.419	5.9
P10-19	97.063188	59.515637	0.0045667		0.01755	1.54	19.139	12.94
P10-20	97.155741	55.436103	0.0028877		0.01673	1	21.115	14.03
std	462.31223	105.77796	0.0269261		0.07129	1	16.801	1.12
P10-21	44.67801	165.91485	0.0061596		0.02498	1.83	4.74	5.99
P10-22	120.89146	48.208908	0.0045334		0.01695	1.87	21.116	11.49
P10-23	304.97159	158.97757	0.0076568		0.02251	1.41	19.82	2.71
P10-24	152.74663	78.587975	0.0042331		0.01615	3.78	20.149	5.46
xx	294.62245	1221.0853	0.0062987		0.01846	2.08	6.301	8.21
std	431.83695	116.67053	0.027843		0.07023	1	16.58	1.68
P10-26	1249.3267	710.17023	0.00744		0.02186	2.16	19.77	1.12
P10-27	136.27214	84.531255	0.0051194		0.01707	1.46	18.704	6.4
P10-28	301.18532	202.21649	0.0050571		0.01725	1.64	20.142	2.67
P10-29	38.056241	12.487101	0.0106012		0.02342	2.3	34.515	90.51
P10-30	2084.8139	1256.5586	0.0068393		0.02026	2.09	19.849	1
std	472.28275	98.219438	0.0268692		0.07098	1	16.786	1.6
xx	1122.453	769.54091	0.005782		0.02124	9.58	14.99	55.04
P10-32	294.87487	171.15405	0.0077636		0.02167	1.71	19.381	2.92
xx	38.805082	146.36622	0.0089834		0.02222	1	13.586	19.79
xx	85.350986	8.7389	0.0003994		0.0162	2.13	11.919	10.61
xx	295.77516	10.250605	0.015962		0.01738	3.17	10.864	4.05
std	483.74253	86.105086	0.0283999		0.06918	1	16.87	1.05

P10-36	624.49088	454.25713	0.0062885		0.02006	1.23	19.722	1.58
P10-37	156.40669	88.983539	0.0043816		0.01585	1.15	19.29	5.76
P10-38	189.3725	153.57271	0.0051704		0.01646	2.02	21.612	6.55
xx	366.09885	463.63799	0.00634		0.0173	1	7.015	5.96
std	470.16244	88.983539	0.0287271		0.0698	1	16.793	2.34
P10-40	0.0168279	0.0207083	0.9979452		-0.01816	1	2.767	237.2
std	619.34155	177.0145	0.0230267		0.06971	2.04	16.836	1.6
std	442.62362	117.99586	0.0289017		0.07063	1	16.711	1.59

IGNEOUS ZIRCON

xx = indicates discordant data

Spot Name	ppm U	ppm Th	238Th /232U		Total 238 /206	% err	Total 207 /206	% err
xx	374.84297	109.8895	0.020363		0.06488	1	17.184	5.62
std	596.24814	138.9914	0.0264379		0.06597	1.62	16.89	2.51
std	312.12742	69.373296	0.0232337		0.068	1.07	16.868	1
std	393.67024	92.171314	0.0264231		0.06975	1.79	16.473	4.1
std	547.53143	115.15294	0.028941		0.07073	1	16.621	2.48
std	520.45258	136.7269	0.0275536		0.07048	1	16.815	2.61
xx	89.929522	28.979493	0.0076467		0.02117	1	13.494	11.77
xx	46.707861	18.207813	0.012708		0.02611	1.03	9.07	8.51
xx	299.73204	185.9645	0.0088796		0.02447	1.4	18.126	3.71
P26-4	1269.6881	1249.4538	0.0103942		0.02199	2.6	19.059	5.91
std	787.82694	226.45011	0.0310765		0.06768	1	16.937	1.77
P26-5	274.54493	108.72665	0.0086964		0.02147	1.31	18.861	7.59
P26-6	231.83674	88.315542	0.0092041		0.02204	1.48	19.31	2.45
P26-7	573.19598	389.9226	0.0080729		0.02217	1	18.557	2.77
P26-8	805.87049	576.34612	0.0086863		0.02208	1	19.125	2.4
std	486.86076	110.13432	0.0320294		0.07088	1.4	16.5	5.07
xx	240.85402	132.04489	0.0061984		0.0201	2.34	18.552	5.21
P26-9	256.03294	107.04358	0.0098133		0.02116	1	20.203	3.92
P26-11	225.49492	113.53107	0.0085969		0.02135	1	20.22	7.62
xx	111.71151	36.140213	0.009332		0.02074	2.75	18.531	8.08
std	476.8796	98.720006	0.0267423		0.06598	1	16.696	3.82
std	346.31379	78.829118	0.0227779		0.06666	1	16.824	1.63
P26-13	325.16238	225.59327	0.0066946		0.02122	1.55	18.866	6.07
P26-14	402.50735	328.13845	0.007469		0.02139	1	19.68624	2.38
P26-15	240.75492	144.46905	0.0055775		0.02125	1	19.889	5.19
P26-16	289.19237	124.05794	0.0070798		0.02161	1	19.568	3.5
xx	253.8079	115.55076	0.0071731		0.0216	1	19.377	5.37
std	565.29573	134.82962	0.0258511		0.06462	1.41	17.088	1.46
xx	720.94957	485.09285	0.0063327		0.02025	6.31	13.866	15.89
P26-19	536.7125	296.00701	0.0089976		0.02269	1	18.991	2.12
P26-20	143.97011	48.013543	0.0091774		0.02201	1	19.914	8.31
P26-21	239.61988	108.29823	0.0099539		0.02134	2	19.891	7.54

std	506.742	114.99993	0.0333252		0.0682	2.02	16.709	2.36
P26-22	192.32648	85.469615	0.007395		0.02146	2.49	18.969	5.86
P26-23	370.32983	207.35485	0.0108712		0.02174	1	19.647	6.27
P26-24	437.62158	207.59967	0.0116801		0.02218	1.29	19.139	3.86
P26-25	200.15467	89.019373	0.0098337		0.02188	1	19.645	4.47
xx	457.18753	96.669715	0.0365537		0.07273	1.23	16.634	5.65
P26-26	1059.7865	857.66448	0.0085378		0.02156	1	19.939	2.19
std	499.08498	112.18461	0.026215		0.06756	1	17.14	2.25
P26-27	319.1899	187.67818	0.0080619		0.02289	1.04	18.651	6.23
P26-28	424.22628	303.65735	0.0083186		0.02156	1	19.464	1.9
xx	3219.3111	2601.2079	0.0084825		0.0236	1.26	18.4	8.6
P26-29	175.36392	69.587506	0.008786		0.02273	1	18.499	7.51
std	514.24589	104.74848	0.0272043		0.06799	1	16.454	1.83
P26-31	558.44945	387.38269	0.0082159		0.02172	1	18.128	5.06
P26-32	367.08685	170.78622	0.0082356		0.02124	1.04	19.037	5.24
xx	639.01038	407.33478	0.0061637		0.0229	1	11.235	18.85
P26-34	595.83376	390.47343	0.0072185		0.02353	1.2	19.133	3.81
std	582.4745	127.11807	0.0236311		0.06437	1.14	17.143	3.26
P26-35	387.88694	209.68056	0.0098821		0.02142	1.01	19.278	5.37
xx	353.44834	176.69229	0.0079277		0.02233	2.8	17.165	6.59
P26-37	242.29534	136.45149	0.0072953		0.02276	1	18.293	4.65
P26-38	637.22674	336.58442	0.0081014		0.02205	1	18.567	2.58
std	469.33067	113.16385	0.0296895		0.06755	1.21	16.725	3.2
P26-39	235.48509	120.17156	0.0061687		0.02109	1.5	18.848	5.28
xx	86.758612	13.801216	0.002422		0.02121	1.14	14.798	12.21
std	573.02483	141.92913	0.0294656		0.06863	1	16.814	1.98
P04-1	200.17268	87.795319	0.0070773		0.0222	1	20.446	7
P04-2	301.22742	170.69442	0.007847		0.02165	1.91	19.435	4.69
xx	463.4753	264.02858	0.0069762		0.02182	2.46	17.448	9.18
xx	385.48173	195.54273	0.0048349		0.0233	1	15.777	20.22
std	524.65944	106.82937	0.0262267		0.06541	1.34	16.813	3.1
P04-5	305.7856	188.87163	0.0076942		0.02166	2.55	18.987	3.45
P04-6	273.81526	129.71919	0.0071066		0.02172	1	19.329	3.12
P04-7	282.12088	109.06327	0.0073222		0.02184	1.05	19.753	3.4
P04-8	184.45326	106.64576	0.0065452		0.02179	1.79	19.925	5.64
std	531.78498	107.625	0.0270216		0.06614	1	17.02	3.37
P04-9	510.89481	374.83613	0.0063776		0.02181	1	19.57	2.1
P04-10	311.96527	183.11857	0.0063703		0.02076	1.73	19.73	4.43
P04-11	195.7226	95.506863	0.0060644		0.02156	1.65	19.975	7.22
P04-12	320.8294	204.14171	0.0060756		0.02199	1	19.918	4.38
std	469.5739	111.29717	0.0291772		0.06949	1.39	16.551	4.35
std	586.53723	138.44058	0.0309583		0.0676	1	17.074	3.14
xx	473.78076	226.72552	0.0067581		0.02254	1	17.214	3.75
P04-14	615.94021	374.1935	0.0068479		0.02114	2.44	19.56	4.23
P04-15	441.54017	323.73185	0.0066762		0.0215	1	19.933	3.6
P04-16	206.46946	98.322188	0.0073507		0.02205	1.23	18.572	5.44
std	438.1891	102.63698	0.0283907		0.07105	1.01	16.566	3.59
P04-17	283.5532	119.37593	0.0069102		0.02134	1.19	19.568	3.33

std	478.11373	96.883924	0.0264703		0.06751	1.31	17.007	2.65
P04-18	390.5714	202.42803	0.0079484		0.02206	1.77	19.972	3.81
P04-19	366.62743	192.05417	0.0073307		0.02144	1.64	19.188	5.93
P04-20	346.50296	146.94776	0.0075413		0.02224	1.87	20.038	2.75
P04-21	537.72143	375.72357	0.0064075		0.02198	1.92	19.59	3.1
std	472.11423	96.180093	0.0266031		0.06907	1	16.878	4.22
P04-22	361.96115	226.2053	0.0060248		0.02214	1	19.666	3.23
P04-23	372.74404	195.48152	0.0062205		0.02209	1	19.129	4.94
P04-24	347.33172	178.25296	0.0068453		0.02219	1	19.8	4.35
xx	340.63858	170.57201	0.0069776		0.0222	1.93	18.376	28.34
std	631.70467	157.22982	0.0297823		0.06709	1	16.911	1.74
xx	239.53881	97.832567	0.0101709		0.02185	1	18.226	13.03
xx	111.40523	36.201416	0.0093342		0.02192	1.14	16.248	18.13
std	535.3973	110.99115	0.026226		0.0665	1	17.054	5.62
std	539.17176	106.58456	0.0266369		0.06541	1	17.072	4.26
std	600.64417	135.77826	0.032962		0.06704	1	16.866	1.82

Spot Name	ppm U	ppm Th	238Th /232U		Total 238 /206	% err	Total 207 /206	% err
std	684.70844	239.09662	0.0195752	1.031	0.089888	1.84	16.995357	2.76
std	500.76344	138.19522	0.0276651	4.294	0.095111	2.49	16.805094	2.5
std	443.81623	98.40967	0.0303561	2.227	0.092124	1.46	17.133679	2.99
std	349.95803	51.504894	0.0329252	1.589	0.087398	1.28	16.831516	2.891
std	530.94486	101.2026	0.0275577	3.784	0.09286	1	16.996336	1.6
P24-1	937.40282	1439.6453	0.0016072	61.13	0.030561	1.58	18.642738	3.895
P24-2	325.27616	158.92313	0.0065966	5.853	0.028477	1	20.524567	2.964
P24-3	719.39318	396.40423	0.0084215	1.4	0.029831	1	19.494061	3.277
P24-4	857.44088	517.9514	0.0082919	1.531	0.029774	1	20.286812	2.071
std	678.52781	162.26369	0.0233408	5.163	0.093779	1.36	17.004476	1.52
P24-5	2682.5981	2734.3047	0.0074241	3.675	0.029027	1	19.565468	2.511
P24-6	843.33114	587.77462	0.0065288	4.88	0.029351	1.6	20.311403	2.133
P24-7	1235.7099	969.50228	0.0082818	1.566	0.030718	1	20.294192	2.481
P24-8	2163.6689	1678.5229	0.008299	1.326	0.029188	1.28	20.144817	2.261
std	394.41182	61.69087	0.030419	2.895	0.09098	1	17.035628	1.85
P24-9	1163.2602	793.1918	0.0089736	1.921	0.029057	3.25	20.132494	1.64
P24-10	1327.9314	1106.2189	0.0089991	1.685	0.029483	1	19.375605	1.704
P24-11	1275.3452	987.21821	0.0087914	3.681	0.030122	1.27	20.29784	2.68
P24-12	1012.9428	813.18041	0.0088068	1.444	0.029625	1	20.149657	2.62
std	463.14087	79.653236	0.0314292	2.092	0.088364	1.56	16.753894	2.731
P24-13	700.33284	464.66669	0.0096707	1.95	0.029011	1.54	20.115616	3.611
P24-14	576.46604	307.08527	0.009288	3.217	0.029987	2.27	19.482481	5.33
P24-15	626.31772	361.30095	0.0104776	3.462	0.029545	3.21	17.37379	12.93
P24-16	625.29101	423.4573	0.0100825	1.347	0.028983	1.41	20.055214	3.453
std	454.56118	93.727407	0.0315325	1.746	0.090746	2.15	17.0404	2.77
P24-17	2396.0323	2577.6543	0.0083415	7.6	0.029609	1	20.134548	2.21
P24-18	360.25569	159.60767	0.0076571	12.72	0.029521	1	20.315681	3.312
P24-19	1679.7396	1314.3468	0.0077353	9.971	0.02911	2.33	19.840035	2.45

P24-20	800.06671	686.54025	0.0090229	1.122	0.03011	5.17	19.50796	2.412
std	496.69724	125.983	0.0252352	4.144	0.095764	3.31	16.916421	1.591
P24-21	2417.085	2663.6053	0.0095054	4.19	0.030078	1	19.965368	2.38
std	683.41742	195.47764	0.02247	2.769	0.092418	1.97	17.044485	1
P24-22	682.62451	511.84529	0.0065112	5.326	0.027965	2.32	20.487695	2.395
P24-23	3571.2471	3260.8266	0.0076694	1.951	0.029681	3.71	20.192402	1
P24-24	1882.1248	2126.4594	0.0075395	6.011	0.028496	2.41	20.054511	1.151
std	663.01523	185.8393	0.0241561	3.474	0.091912	1.23	17.040389	1.31
P24-25	1857.3006	2462.1585	0.0084451	1.161	0.029658	1.88	19.936542	1.9
P24-26	73.527172	34.309214	0.0052981	10.71	0.022228	2.27	21.440258	6.043
P24-27	2144.5476	2320.431	0.0082277	1.712	0.02892	1.38	20.217073	2.061
P24-28	1851.4453	1861.7883	0.0077152	3.15	0.029357	1	20.286232	3.07
std	466.07871	99.477555	0.0302131	5.112	0.088902	1.47	16.949646	3.52
P25-1	1072.2992	448.31985	0.0079387	4.31	0.029157	1	20.144538	1.251
P25-2	60.27134	8.6252215	0.0096483	43.89	0.032762	1.49	5.9523449	19.28
P25-3	1357.1268	691.90705	0.0065273	4.841	0.029205	1	19.841328	1.292
P25-4	1034.4123	537.22808	0.0067765	2.265	0.030401	1	20.135348	2.411
std	354.44102	61.827778	0.0279854	2.12	0.091296	1.93	16.906493	2.3
P25-5	1053.2185	473.26453	0.0086176	1.524	0.02955	1	19.81232	1.991
P25-6	299.20161	101.77761	0.007674	6.268	0.029455	1	20.843451	4.741
P25-7	1445.4854	792.39773	0.0084	2.497	0.029587	1	20.406284	1.761
P25-8	396.32294	185.09999	0.0073636	12.05	0.030378	1	20.337944	3.336
std	532.74416	108.59565	0.0284062	2.704	0.092055	1.07	16.994823	2.19
P25-9	610.20538	267.6283	0.0082973	2.326	0.029107	1.12	20.223074	2.953
P25-10	746.43345	318.88676	0.0085576	1.976	0.029137	1	20.352162	2.621
P25-11	841.64367	373.07506	0.0088644	3.304	0.028577	1	20.193401	2.271
P25-12	1346.1988	688.34744	0.0095591	1.361	0.029908	1.73	20.090371	2.311
std	422.11285	80.009198	0.0275791	4.307	0.090548	1.41	16.916083	5.57
P25-13	1168.0279	531.39579	0.008961	1.952	0.030045	1.06	20.626463	3.301
P25-14	873.60405	276.5821	0.0081554	8.666	0.029072	1	20.152416	3.77
P25-15	231.56027	65.66121	0.0070834	6.504	0.029221	1.14	21.464639	6.657
P25-16	887.52064	379.37284	0.0074813	5.489	0.029732	2.77	19.346627	3.582
std	354.30887	58.240781	0.029114	1.093	0.092482	1	16.855803	2.94
P25-17	584.42564	222.06523	0.0080531	3.938	0.029239	1.16	20.003208	3.983
P25-18	1562.6023	806.7731	0.0078287	6.74	0.030669	1.09	20.057594	2.27
P25-19	1998.0422	1204.2726	0.0085031	3.615	0.030165	1	19.60577	2.77
P25-20	246.79838	156.26711	0.0073001	5.4	0.029284	1.81	20.539304	3.007
std	765.89025	165.02924	0.0263393	4.244	0.091047	1.3	16.96464	1.73
P25-21	848.50539	428.30386	0.0082527	2.292	0.02984	1	20.12175	1.514
P25-22	955.17214	566.66336	0.0073349	8.468	0.029598	1	20.392058	5.91
P25-23	1099.0548	567.15623	0.0086742	9.496	0.029726	2.22	16.410158	4.765
P25-24	1148.7845	533.66847	0.0080392	10.14	0.029459	2.98	19.990773	2.062
std	412.78091	88.032023	0.0301573	2.897	0.096572	1	17.044178	2.81
P25-26	1178.5695	514.91203	0.0072358	10.92	0.029061	1.97	20.088356	3.57
P25-25	1372.7105	740.31782	0.0072486	9.704	0.02935	1.76	19.129075	3.103
std	697.1612	119.79474	0.0281786	4.705	0.090012	1	17.073264	1.38
std	384.26664	98.546578	0.0254224	2.804	0.091028	4.54	17.074256	4.231
std	662.25282	183.40233	0.0231093	2.221	0.091819	1.89	16.905848	1.12

